BUDAPEST UNIVERSITY OF TECHNOLOGY AND ECONOMICS

FACULTY OF MECHANICAL ENGINEERING

DEPARTMENT OF MACHINE AND PRODUCT DESIGN

ENGINEERING OF FRACTAL VISE:

DESIGN AND INTEGRATION OF A HYBRID FRACTAL – BENCH VISE FOR ADAPTIVE CLAMPING OF IRREGULAR WORKPIECES

Author:

Muhammad Kevin Fahlevi

Supervisor:

Dr. Baka Ernő Zsolt

Gábor Vincze

INNOVATION STUDENT'S CONFERENCE (IDK)

Budapest, 2025/26/1

TABLE OF CONTENTS

1. ABSTRACT

The industrial vise has seen increased variations in recent years to improve tool-clamping efficiency and durability. The Bench Vise, commonly used in machining and assembly, for the purpose of workpiece-clamping in place. However, it often struggles with irregular or complex shapes of components, resulting to the inefficiency of gripping force and potentially causing uneven stress, deformation, and surface damage.

To overcome these challenges, this paper introduces a mechanically hybrid vise system combining the adaptive clamping of a Fractal Vise with the foundational structure of a Bench Vise. Using self-repeating arc geometry, it creates multiple contact points that adjust to complex shapes and distribute uniform pressure. A dovetail mechanism enables sliding motion, pushing the smallest arc to clamp objects.

The design process involves CAD modelling using *PTC Creo* while considering the application of DFM and DFA principles, *PET-G CF* for the additive manufacturing (3D printing) of the main fractal bodies, as well as *Aluminium* for the subtractive manufacturing (milling and drilling) of the mounting interface, the connection plates between the Bench Vise and the Fractal Vise. Additionally, a prototype is produced using *Bambu Lab X1 Carbon Combo*, followed by mechanical testing and structural analysis to evaluate the clamping's performance, durability, and industrial usability.

Keywords: Fractal Vise, Bench Vise, Hybrid System, Adaptive Clamping, Irregular Workpieces, CAD Modelling, DFM/DFA, Additive Manufacturing, Substrative Manufacturing, Prototyping.

2. THE TECHNICAL AREA

2.1 Principle of Fractal Vise

Fractal Vise is a unique industrial clamping tool that uses fractal-based geometry to adapt to the object it grips. As shown in Picture 1, it showcases a custom contact surface made of circular arcs that adjust to the workpiece's shape. Similar to the characteristics of fractal geometry, its design follows an iterative, self-repeating pattern which built from arcs, gradually decrease in size and dimension **[1]**. By applying the tapering curvature, the vise could strongly hold objects while applying even and gentle pressure; suitable for handling parts with diverse shapes.

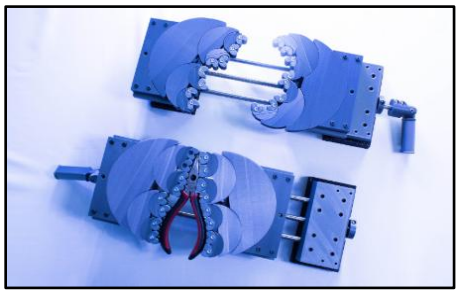

Picture 1. Fractal Vise with and without examined workpiece

The main semi-circle body of Fractal Vise applies to a series of concentric arcs, where each arc is about half the size of the arc prior to it, as shown in the figure below. When the outer jaws exert force to the workpiece, the sliding dovetail joints enable each arc to rotate and conform to the natural shape of the object.

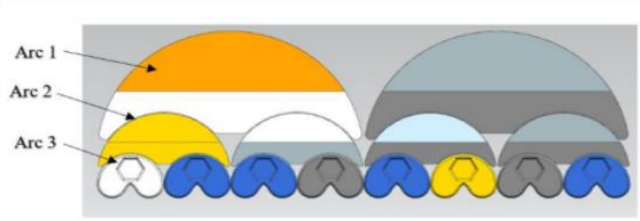

Picture 2. Different series of arcs of fractal bodies

The vise system consists of ten essential parts. The operation begins with the user rotating a crank (1), converting rotational motion through the nut into liner motion via a lead screw (2). This drives a half-rectangular block (3), containing the dovetail mechanism forward. Components

(8) and (3) are symmetrical, connected by arcs of equal diameter. When the smallest arc (6) contacts the object, the connected parts (3), (4), (5), (6), and (7) follow the movement through the groove system and shape themselves to fit the workpiece's surface precisely **[2]**.

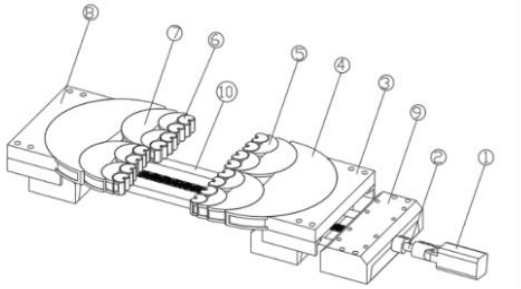

Picture 3. Mechanical structure of the general Fractal Vise

To keep the object securely in the gripping area, the generated friction force between the vise and the examined component must be larger than the part's weight (W). This friction force relies on the clamping force (F_h) applied by the vise. The clamping conditions must meet the following requirement:

$$Ff = \mu N = \mu Fh > W$$

Where W is the workpiece's weight and F_f is the friction force. The coefficient of friction denoted by μ is 0.2.

Since the manufactured Fractal Vise is used for relatively small or medium-shaped tools, the average mass of the examined workpiece is about 1-2 Kg. 2 Kg mass equals to *19.62 N* weight, as calculated by the following equation:

$$W = M \cdot g, \qquad W = 2 \cdot 9.81 = 19.62\ N$$

With the *19.62 N*, the minimum clamping force F_h must be greater than *98.1 N* or rounded to *100 N*. The vise will also experience a reaction force $N=F_h=100\ N$ and the friction force F_f is calculated **[3]**:

$$Ff = \mu N = \mu Fh = 0.2 \cdot 100 = 20\ N$$

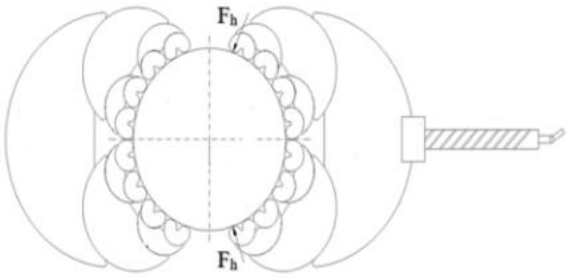

Picture 4. Clamping model

Consider *PETG – CF* is the material used to produce the fractal components, the tensile strength at yield σ_y is *57.6 MPa* (ISO 527). Given the safety factor (SF) for the 3D printed parts (anisotropic, layer based) of 2 is standard, the allowable stress σ_{allow} can be obtained by:

$$\sigma allow = \frac{\sigma y}{SF} = \frac{57.62}{2} = 28.8 \sim 29\,MPa$$

The minimum cross-sectional area A of the clamping jaw is determined as follows:

$$A = \frac{N}{\sigma allow} \cdot SF = \frac{100}{29} \cdot 2 = 6.9\,mm2$$

A represents the contact area between the fractal jaws component and part. The cross section of this component is shown below:

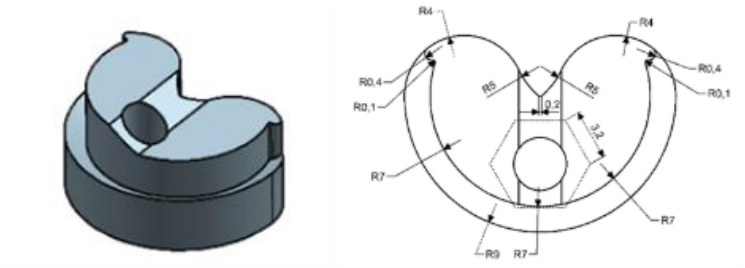

Picture 5. Clamping jaws component

2.2 Classification of Fractal Vise

Currently there are various type of Fractal Vise design variations in the market, which each manufacturing or maintenance shopfloor might use different design or models depending on their application and scalability. In terms of design features, Fractal Vises can be categorized based on their power mechanism, jaw's structure, and tooth design.

2.2.1 Classification Based on Power Mechanism

The mechanism of clamping force generation is one of the key differences among Fractal Vises. Similar to a standard Bench Vise, the first type of driving mechanism applies a rotating handle. In general, the clockwise direction is used to turn the handle which drives a lead screw, converting rotational input from the user into a linear motion to the vise jaws **[4]**. Considering its simplicity, easily controlled, and efficient for industry installation; from light-duty clamping to heavy machining, depending on the material used, this power mechanism approach is universally applied among the industry.

Another power-mechanism variant is the gear-driven Fractal Vise; applied interlocking gears system instead of a lead screw. The fractal jaws clamp and move together in synchronize motion while the user rotates the gear. Practically in the compact design, the user can exert less effort with the higher torque transmission. This approach is significantly advantaged in automated or high-precision environments.

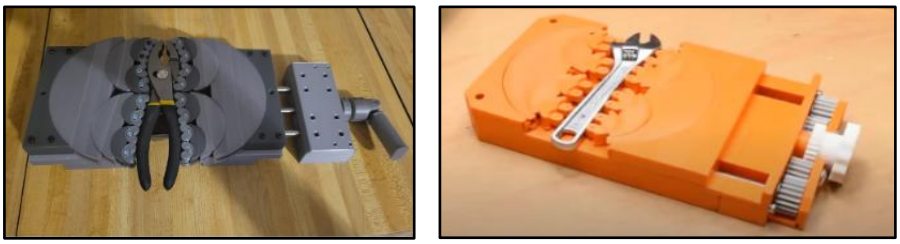

Picture 6. Rotating handle (left) and rotating gear (right) Fractal Vises

2.2.2 Classification Based on Jaw Structure

The jaw structure of a Fractal Vise defines how contact points engage with the workpiece and distribute forces. Common designs use mechanical-bearing types with pivoted joints or pins, which make segments rotate and adapt to various shapes **[5]**. These systems offer strong grip and rigidity while minimizing wear in tight areas, especially around metal components.

Alternatively, flexure-based jaws applied flexible elements that bent slightly to match surface contours. While lightweight and low maintenance ideal for delicate tasks, these jaws present less clamping force and can fatigue over time which lead them more suitable for low-load applications.

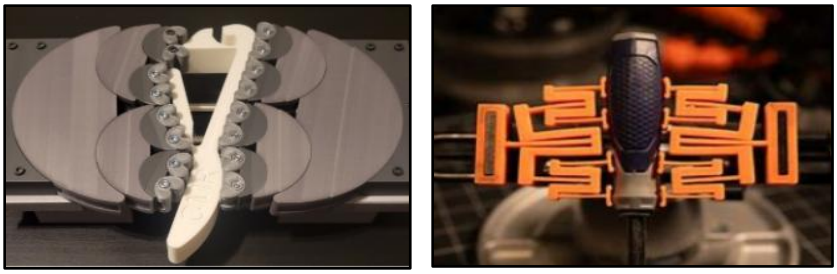

Picture 7. Mechanical bearing jaws (left) and flexure jaws (right) of Fractal Vises

2.2.3 Classification Based on Teeth Design

While mechanical bearing jaws are selected for industrial use, the teeth design also serves a key role and is relevant to the target workpiece. The first type, flat-surfaced teeth, is ideal for rectangular or cubic objects. It is easy to produce and cost-effective which suitable for flat-surfaced metalworking, though less efficient for irregular shapes. The second type uses C-shaped jaws, designed for cylindrical objects like pipes and tubes **[6]**. Their concave form prevents rolling or slippage while increasing the contact area for better grip.

The third and most versatile jaw design is the curved type with semi-circular profiles. It creates multiple contact points, adapting naturally to various shapes – flat, round, or curved. This improves vibration control and ensures uniform force distribution. However, its complex geometry makes manufacturing more difficult and costly, for metal-base material as CNC machining is required **[7]**. The performance may be less effective for flat workpieces compared to flat jaws. When made of metal, increased joint movement can also lead to higher long-term wear.

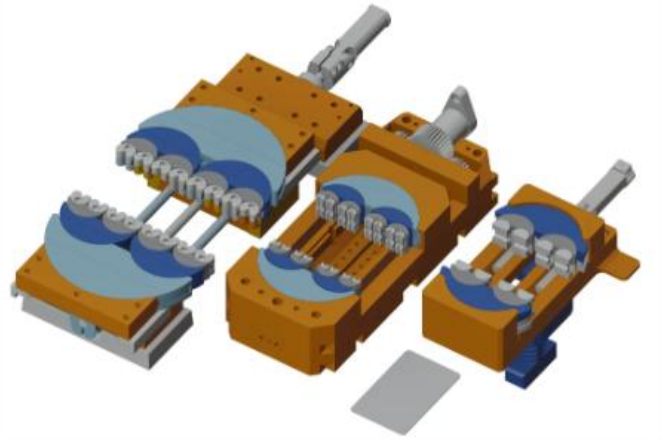

Picture 8. Various teeth designs of Fractal Vises

3. STATE OF TECHNOLOGY

Selecting the right type of vise is crucial in industrial applications to ensure effective clamping. Common types – such as Bench Vise, Quick Release Vise, and Machine Vise – each offer unique mechanical benefits and limitations. This chapter presents a comparative analysis of these vises against the Fractal Vise, focusing on design, materials, structural mechanisms, ease of installation, and industrial application.

3.1 Bench Vise

Picture 9. Bench Vise

The Bench Vise body is typically made from solid cast iron for strength and durability, which a mild steel spindle handle for manual jaw adjustment **[8]**. It includes basic components like the base, spindle, jaws, and a bolt holes. Idea for machining tasks like filing and sawing, its rigid, flat jaws work well for regular tools but are limited for irregular shapes. All adjustments are manual which time-consuming during repetitive work or tasks.

Compared to the Fractal Vise, the Bench Vise is simpler but less adaptable. It struggles with irregular or rounded workpieces and lacks modularity. The Fractal Vise, designed for hybrid integration, enables more flexible clamping setups and can be customized to fit existing base systems which offer better adaptability and efficient use of space.

3.2 Quick Release Vise

Picture 10. Quick Release Vise

The Quick-Release Vise installed at Atlas Copco Hungary added a mechanism to the standard Bench Vise, resulting much faster clamping and unclamping. Using a buttress-threaded spindle, half-nut, and spring-loaded lever, the jaw slides freely when the lever is pressed and re-engages for normal use when released.

While both the Quick Release and Fractal Vises aim to improve efficiency, their implementation differs. Quick Release Vise is a stand-alone tool ideal for repetitive tasks but limited in adaptability. In contrast, the Fractal Vise offers modular integration into existing vises, focusing on passive adaptation and reducing adjustment time during setup.

3.3 Machine Vise

Picture 11. Machine (Milling/Drilling) Vise

Machine Vises are sued in milling, drilling, or shaping tasks, secured to the machine table with T-bolts for stability under heavy loads. They feature a fixed jaw and a moveable jaw driven by a threaded spindle, with some variants allowing tilt for angled cuts. Known for precision and vibration resistance, they are ideal for flat square objects. However, they are less suited for irregular shapes and are heavy and expensive to produce **[9]**.

When compared to Fractal Vise, the application procedure is highly different. Fractal Vise is not as strong as Machine Vise but offers more flexibility; it easily holds all sorts of shapes due to the unique mechanism of the teeth jaws. In a Machine Vise, users can consistently work on repetitive tasks in a production shop floor, while the Fractal Vise is more applicable when things change often. It's not about replacing the Machine Vise but filling in where the Machine Vise falls short.

4. PROOF OF CONCEPT

This chapter details the development stage of the Fractal Vise system and mounting interface, focusing on prototyping of each unit after the completion of design and manufacturing processes. During prototyping, all individually machined components of the fractal segments and base plates are carefully assembled to the Bench Vise, to form the complete hybrid system and assess its applicability. The goal of this chapter is to evaluate the accuracy of fabrication, fitment of parts, and structural alignment, as a proof of design and modeling concept of this integration model idea.

4.1. Prototyping of Fractal Vise

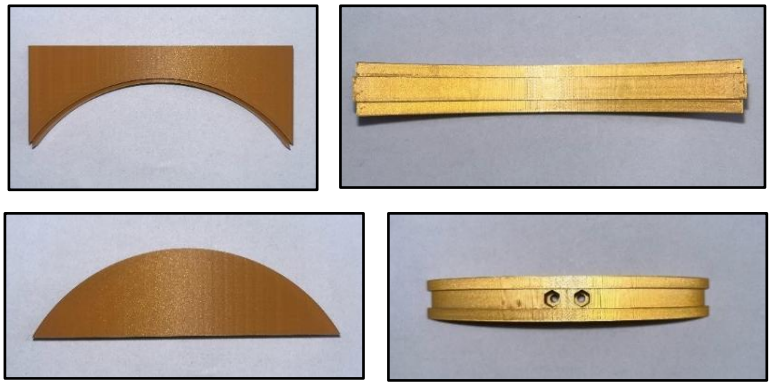

Picture 12. Sample Part 1 (top) and Part 2 (down) - top and front views

To begin prototyping the Fractal Vise, two main parts were produced to test dimensional alignment and fitness, focusing on the dovetail connection. The first part includes a c-shaped dovetail slot and two central holes for M3 hex nuts and bolts. During assembly, bolts are inserted and unscrewed to lock the nuts in place, after which the second component, designed to slide into the dovetail track, is guided into position.

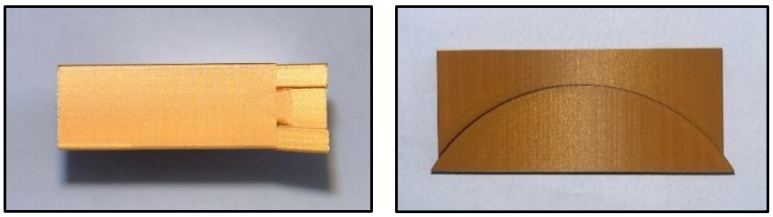

Picture 13. Assembled sample parts of Fractal vise – side (left) and top (right) views

The eight individual components of the Fractal Vise assembly are shown below, each with front (left) and top (right) views, arranged sequentially from top to bottom as Part 1 through Part

8. On the back side of Part 1, three simple flat holes are created with diameter *Ø6.4 mm* and depth 10.5 mm which are aligning to the holes of vertical base plate of mounting interface. Part 2 features two holes, while the remaining parts have a single hole of *Ø3.4 mm* with various depths, smaller shape leads to shorter depths. All parts are connected horizontally with M3 bolt and hex nuts, except for the last two components (Part 8) which are vertically connected through similar fasteners. Furthermore, each part C (part 2, 4, and 6) contains two tiny side holes to insert *1.76 mm* filament sections, which help secure part C and part D together during assembly **[10]**.

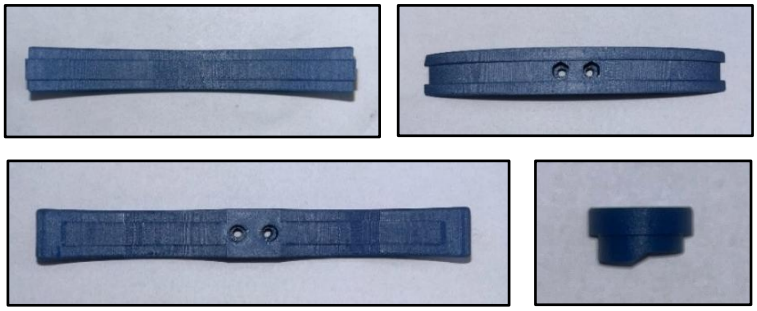

Picture 14. 3D printed Part 1, Part C, Part D, and Part 8

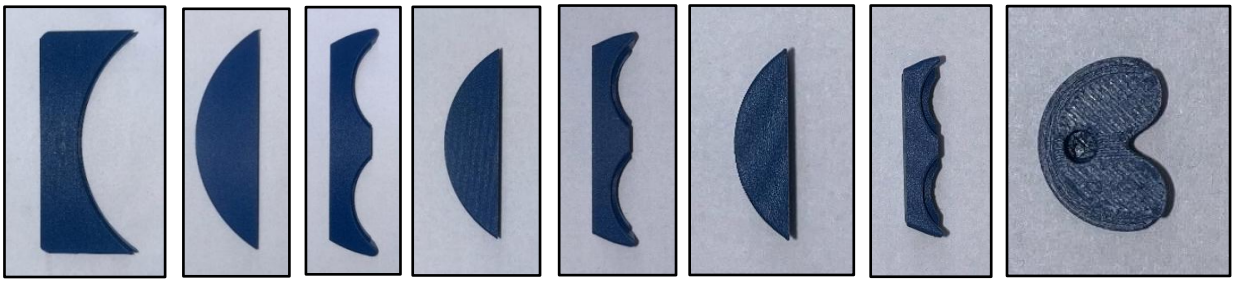

Picture 15. Eight parts of Fractal Vise components – front Part 1 (left) to Part 8 (right)

Following the earlier assembly steps, the half-assembled Fractal Vise was secured in a Bench Vise to stabilize the position while continuing the prototyping of the remaining-half processes. The next stage involved the insertion of M3 bolts and nuts into the designated holes on each part using a manual screwdriver. To reinforce the connection between part C (semi-circular) and part D (arc with dual cutouts), *Loctite* adhesive was carefully applied near the small filament pinholes. This provided additional bonding strength around the interface. Subsequently, to enhance rotational movement along the dovetail tracks, the mating surfaces of each part were deburred with a small file, followed by the application of grease to reduce friction. The parts were then moved back and forth to evenly distributing the lubricant and assessing the smoothness and precision of the sliding fit.

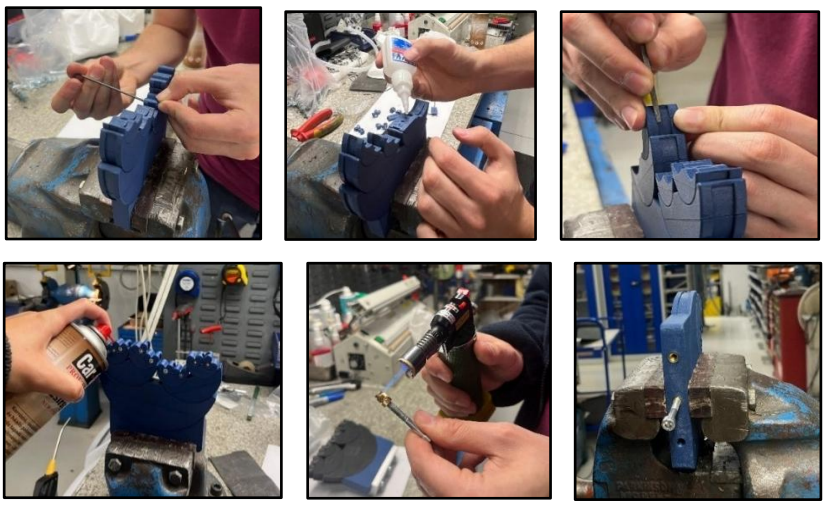

Picture 16. Assembling and prototyping processes of Fractal Vise

The final step involved heating brass inserts with a soldering iron to slightly melt the plastic and later were inserted into the backside of holes of the 3D printed parts. Once cooled, the inserts provided strong threads for bolt connections with the mounting plate **[11]**. The completed Fractal Vise assembly below successfully integrated all eight printed parts, highlighting a full prototyping process that include part validation, manual assembly, lubrication, and threaded insert setting

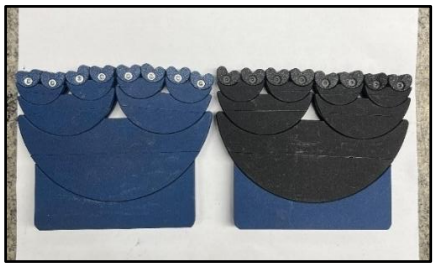

Picture 17. Final prototyping results of Fractal Vise assemblies

4.2 Prototyping of Mounting Interface

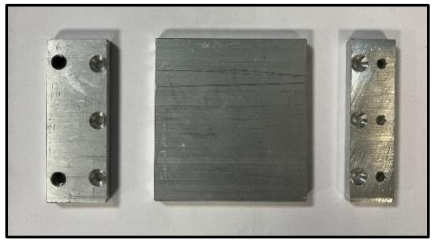

Picture 18. Original base plates of mounting interface

The mounting interface was prototyped by modeling and fabricating three aluminum base plates using milling and drilling machines. These included two vertical and one horizontal plate

with matching widths to support the Fractal Vise. *Ø5.2 mm* holes were drilled and countersunk to fit M5 screws, ensuring secure connection at two points. The parts were then manually assembled using a screwdriver to fasten six screws.

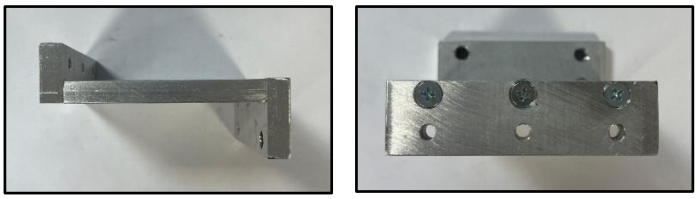

Picture 19. Assembled original parts of base plates - side (left) and front (right) views

In the second development stage, the mounting interface was improved by increasing the number of base plates from three to four. A new horizontal plate was added to partially cover the top of the Fractal Vise, while the third vertical plate was redesigned with six countersink holes and three drilled holes aligned with the insert holes of the Fractal Vise. The final picture shows two completed mounting assemblies, each customized for one unit of hybrid vise.

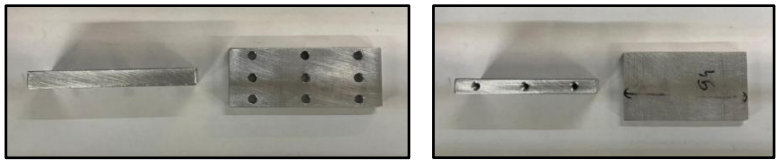

Picture 20. Improved (left) and additional (right) base plates of mounting interface

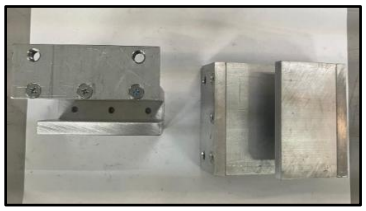

Picture 21. Final prototyping results of mounting interface assemblies

4.3 Final Integration of Prototype Systems

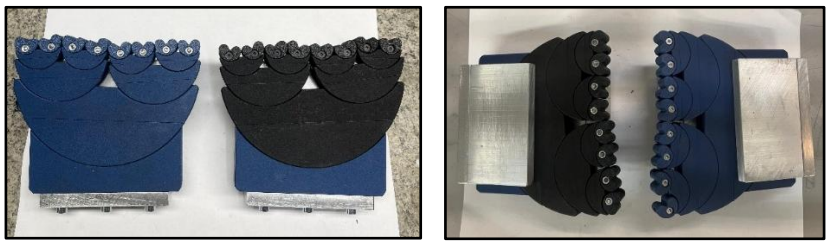

Picture 22. Top and front views of the Fractal Vise and mounting interface assemblies - original (left) and upgraded (right) versions

There are several workshop tools utilized for the final integration process, as displays in the image below (left). Four M8x30 bolts were applied to fasten the mounting interfaces securely onto the vise jaws. Two screwdrivers were employed: the white-handled one was used to remove the original jaws of the Bench Vise, while the red-and-black driver, with its longer shaft, was specifically chosen to insert and tighten the M8 bolts without interference from the horizontal base plate. The right image below shows the actual installation process using these tools.

Picture 23. Installation tools (left) and the prepared Bench Vise (right)

Following the successful installation of the Fractal Vise components and mounting interface plates onto the Bench Vise, the fully assembled setup was ready for functional evaluation. The next phase involved experimental testing, wit a variety of industrial workpieces of different cross-sectional geometries, aimed at assessing the adaptability, grip strength, and overall clamping performance of the system. As shown in the Picture 24, the initial configuration demonstrated the first stage development but revealed some limitations in structural stability during the testing operations. To address this, an upgraded version incorporating additional cap plates was modelled to reinforce the orientation, as depicted in the Picture. This enhancement significantly improved steadiness and structural balance of both fractal components and clamped workpiece, to be in the same straight line of working axis.

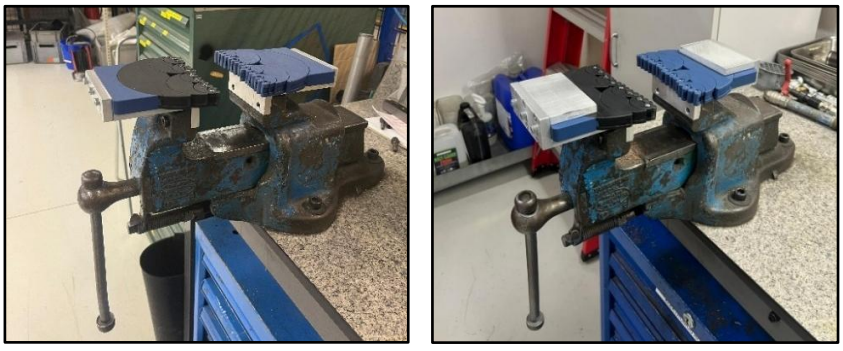

Picture 24. First model (left) and second model (right) of the vise integration assemblies

5. INTRODUCTION TO ILLUSTRATIVE FIGURES AND DRAWINGS

This chapter describe the CAD design and modelling process via *PTC Creo* of full-integration assembly of the hybrid vise system, sub-assemblies' components (e.g. mounting interface assembly and Fractal Vise assembly), and each arc of fractal components which built the main function. The modelling of mounting interface and Fractal Vise was carried out from scratch by considering the installation space on the available Bench Vise at the maintenance shopfloor, meanwhile the CAD model of Bench Vise is taken from the market or engineering catalogue which has the same version to the installed device.

5.1 Vise Integration Assembly

The main assembly demonstrates how the Fractal Vise is integrated into a Bench Vise system using a custom mounting interface. Two models were developed -the original and the upgraded - based on the sub-assembly configuration of the base plates connecting both vises. The initial model used three base plates (two vertical, one horizontal) to connect the Fractal Vise to the Bench Vise **[12]**. While functional for basic tasks, testing revealed that high force caused slight bending in the jaw assemblies. To address this, the upgraded model added a second horizontal plate to cover the top surface and improve stability. This version uses four plates total (two vertical, two horizontal).

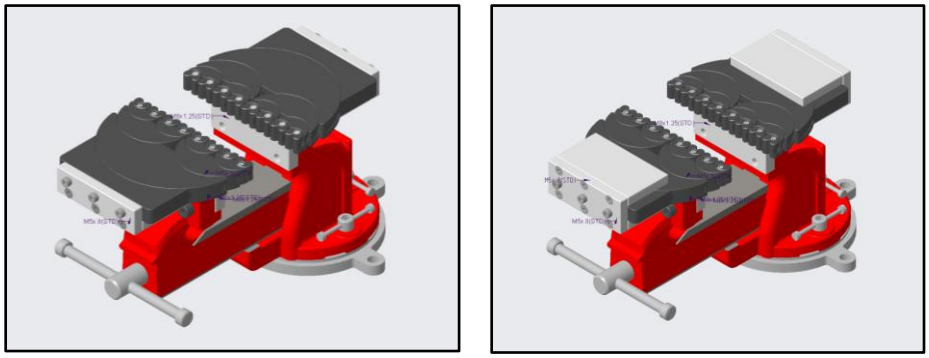

Picture 25. Model 1 - original (left) and model 2 - upgraded of vise integration assemblies

In this vise integration assembly, two types of standardized screws are used to ensure secure connections between the mounting interface components and the Fractal Vise or Bench Vise body. Countersunk screws are used to assemble the base plates; 12 pcs were applied in the first model and 18 pcs in the second or upgraded model. The second screw, counter bore socket head

cap screws are installed for the connection between the Aluminium base plates and the clamping parts of Fractal Vise (M5x16), as well as connection the Bench Vise where higher torque and strength are needed due to the greater load (M8X25). These screws are ISO-standard and are frequently applied in mechanical design due to their high tensile strength and reliability in resisting shear and axial force.

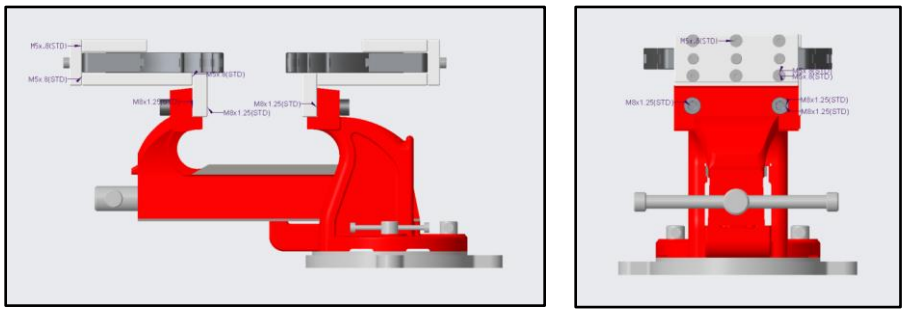

Picture 26. Right and front views of the vise integration assembly – upgraded

The section view (Picture 27) illustrates the fastening system of one-half assembly after all screws are fully installed. On the left, four M5X16 screws attach the main clamping components of the Fractal Vise to the aluminum base plates. As these parts are made from thermoplastic composite (PETG – CF), internal threads from 3D printing are unreliable. To overcome this, heat-set threaded brass inserts were embedded into pre-designed flat holes, acting as strong metallic anchors. Each insert (10 mm long) has an inner diameter of *Ø4.13 mm* for M5 screws and an *Ø8 mm* outer thread to secure tightly to the plastic body. This method improves thread strength and prevents stripping under load. On the right, two M8X25 socket head screws fix the aluminum base to the Bench Vise through threaded holes, ensuring the upgraded assembly's full rigidity.

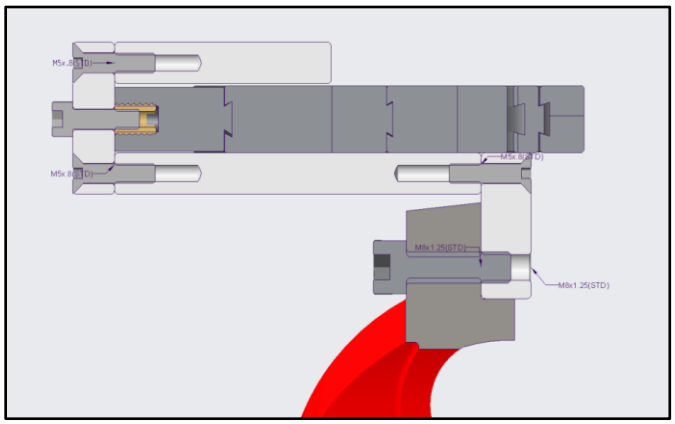

Picture 27. Cross-section view of the screw's connection within the vise integration assembly – upgraded

The exploded view shows the step-by-step assembly of the upgraded vise system, highlighting how each component aligns vertically. From bottom to top, it displays the Bench Vise (red), the mounting interface plates (white), and the Fractal Vise modules (black). This layout helps demonstrate the use of mechanical fasteners to unify materials like cast iron, aluminum alloy, and thermoplastic into one system **[13]**. Each fastener is clearly marked with standard specifications such as M8x1.25 or M5x0.8 for easy reference during assembly.

This view also helps verify screw clearance and overlapping parts, especially in areas with countersinks or tapped holes. It shows how each section relies on the layer beneath, with the interface between the Fractal Vise and aluminum base supported by several screws for proper alignment and strength.

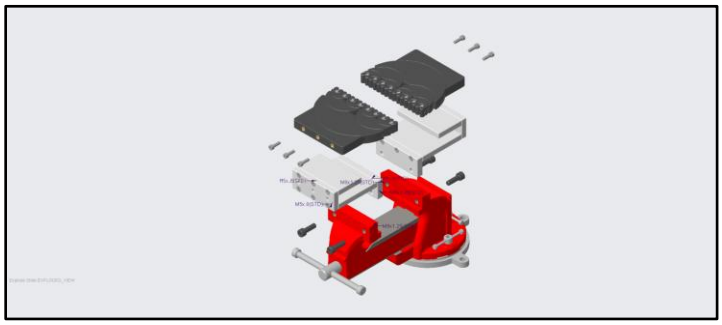

Picture 28. Exploded view model of the vise integration assembly – upgraded

The final assembly drawing below shows a total length of *350 mm*, with a working platform span of *295 mm*, representing the maximum lateral coverage of the Fractal Vise jaws. The height from the base to the jaw surface is *182 mm*, while the Bench Vise height is *141 mm*. The front-end footprint measures *325 mm* from base to driving handle.

The orthographic view on the right highlights the Base Plate with six M5x16 screws in two rows for balanced load distribution. The side view shows a *50 mm* clamping area, though in practice, this varies between *100–150 mm*, depending on how far the movable jaws of the Bench Vise are opened. At the Atlas Copco shop floor, the average spacing is about *161 mm*, with a width of *130 mm*. The screw count includes six M5x16 and four M8X25 pieces.

The 3D rendering in the bottom-left corner of the drawing gives a visual correlation between the components, making it easier to interpret how each element fits and aligns in physical space. All dimensions and scale values (2:5 for the main drawing and 1:5 for the 3D isometric view) are defined based on standard A4 drawing practices using *Creo* software.

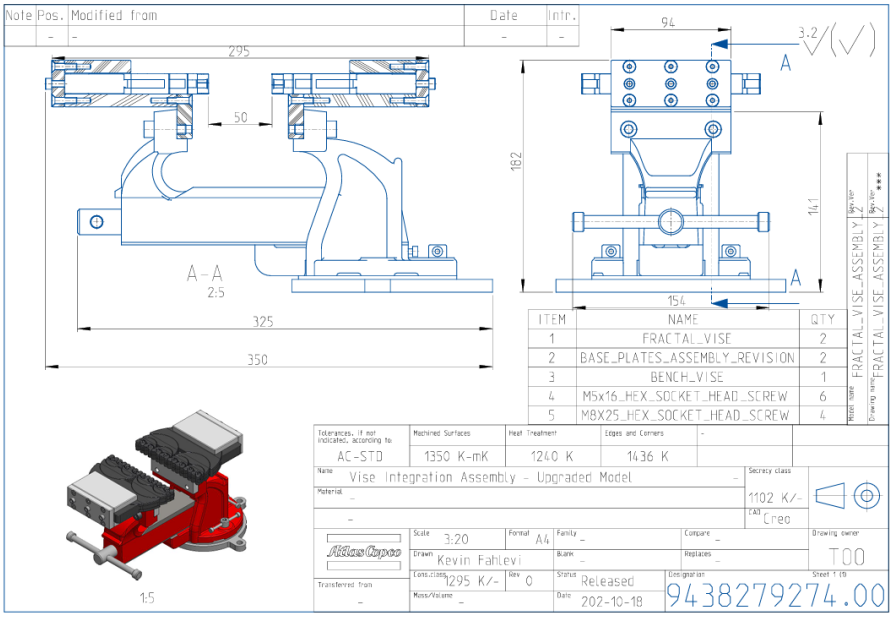

Picture 29. Assembly drawing of the vise integration assembly – upgraded

5.2 Mounting Interface Assembly

The mounting interface connects the Fractal Vise clamping components to the Bench Vise's support base and drive system. This component is important in dividing the integration assembly into two variants: the first using three base plates, and the upgraded version using four. All base plate dimensions were estimated using direct measurements from the Bench Vise at the shop floor with a digital caliper.

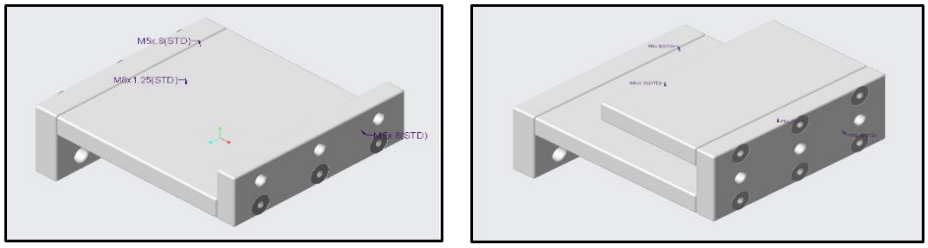

Picture 30. Model 1 (left) and model 2 (right) of mounting interface assemblies

The second model includes a horizontal cap that covers half the Fractal Vise platform, providing enough support to maintain stability under high loads. Each base plate is fastened with M5x20 countersunk screws, using three screws between two plates at evenly spaced intervals. As seen in the exploded view, the system uses 9 countersunk screws in total for one mounting unit to

create a rigid unit -excluding those for mounting the Fractal Vise itself. The countersunk heads ensure the screws sit flush with the surface, avoiding interference during clamping.

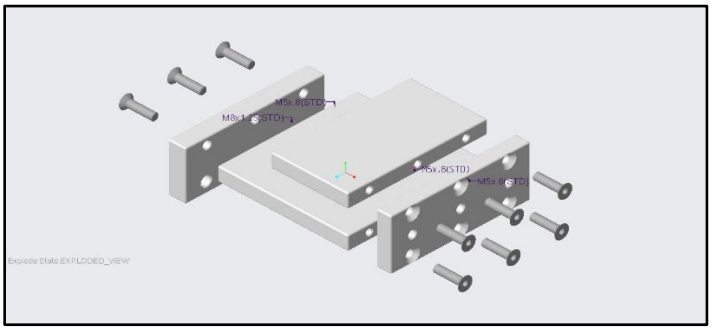

Picture 31. Exploded view model of upgraded mounting interface assembly

The design of vertical base plate 1 as a connecting plate to the Bench Vise exemplifies the modelling approach used for all base plates in this assembly. The design process began with a simple rectangular base profile created using *Sketch 1* with *94 mm x 12 mm* and extruded to *35 mm* tall. Following this, two main sets of features were added: simple-drilled and counter-sink holes (Ø5.2 mm) to connect with the horizontal base plate using M5 screws, and two threaded holes of M8x1.25 to fasten the assembly directly to the Bench Vise. Threaded specifications were defined using the ISO standard with sufficient depth. For safety, 1 mm rounds and *0.5 mm* chamfers were applied to sharp edges, while a groove cut was modeled for mechanical alignment. Since all other base plates in the assembly follow a similar modeling methodology – defined by sketches, extrusions, and hole features – this plate is presented as a representative example to illustrate the overall design process used.

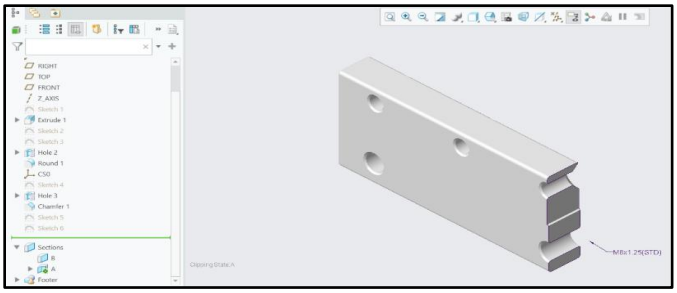

Picture 32. Model of base plate 1 – half view half cross-section

The upgraded mounting interface drawing highlights key geometric features, especially the three *Ø5.2 mm* drilled holes positioned in pairs to fit M5 screws and align the Fractal Vise. A second set of holes, M8x1.25 STD with *Ø6.8 mm*, is used to secure the base plates to the Bench

Vise, aligning with its rectangular jaws. These holes ensure firm attachment using the original screws from the Bench Vise.

The part has a total length of *110 mm* and height of *61.5 mm*. Each base plate has a different height to accommodate the Fractal Vise and Bench Vise jaws. The first vertical base plate is *35 mm* high, while the third is *36.5 mm*. A *0.5 mm* tolerance was included to allow smooth sliding of semi-column parts. Each plate has a thickness of *10 mm*, and the full assembly weighs *489 grams*, light yet strong due to the use of *Aluminum 99.5*.

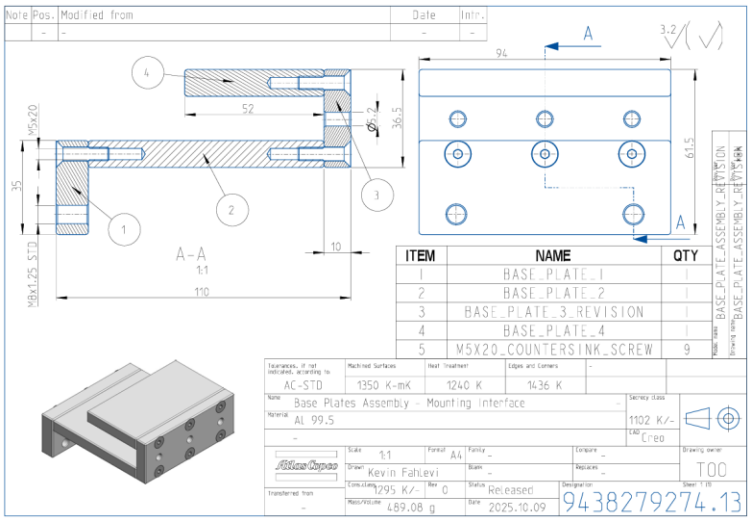

Picture 33. Assembly drawing of upgraded mounting interface assembly

5.3 Fractal Vise Assembly

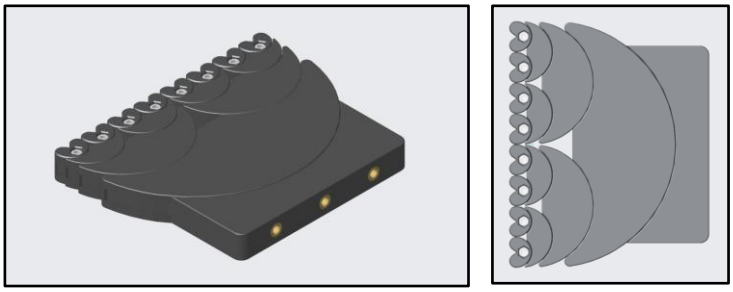

Picture 34. Isometric (left) and top (right) views of a Fractal Vise main components

The clamping jaws components in the Fractal Vise model below build up from a series of concentric arcs and a rectangular block as the side part connected to the vertical base plate of mounting interface. The semi-circular components are reduced by half-diameter to the next arcs in direction to the end of jaws teeth. From the figures below, the parts are categorized into four

distinctive shapes: the first is a rectangular block with a single concave cutout; the second is a half-circle piece, referred to as Part C; the third is an arched profile with two concave cutouts, known as Part D; and the fourth is the eight part, which is symmetrical in both top and bottom views and functions as the clamping teeth. At the final assembly model, two sub-assemblies of Fractal Vise are used in which each of them is placed at the horizontal base plates on the fixed-and moveable jaws of the Bench Vise.

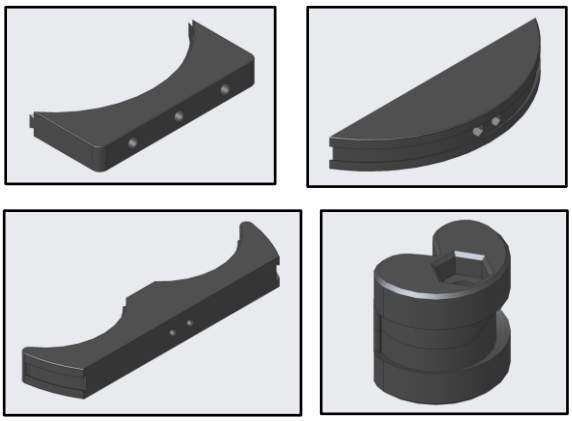

Picture 35. Isometric (left) and top (right) views of a Fractal Vise main components

The modeling process began with designing each individual fractal part, followed by assembling the components with standard fasteners and threaded inserts. Followed by the assembly model, the exploded view was created to show the sequence and hierarchy of components, making the assembly structure easier to understand. This exploded view reveals how each fractal component is positioned relative to the others, alongside the fasteners, bolts, nuts, and threaded inserts required for proper alignment and fixation.

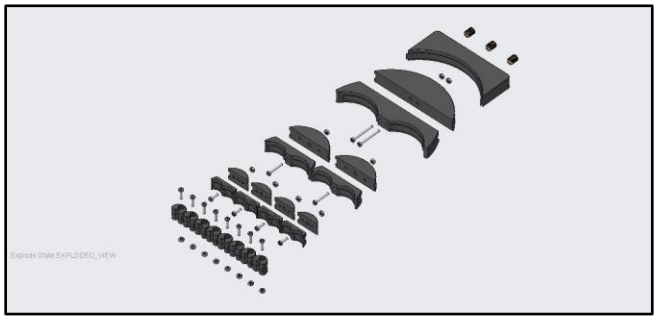

Picture 36. Exploded view model of the Fractal Vise assembly

Dovetail sliding mechanisms support the motion between parts around arcs. The connection between Part 1 (male dovetail) and Part 2 (female dovetail) uses a clearance fit (RC-type), to move or slide relative to the other with minimal friction but without excessive looseness. The male

dovetail width is *2.758 mm*, while the female groove is *1.918 mm*, creating the necessary clearance. Similarly, the 8 mm height of the male dovetail is slightly smaller than the *8.6 mm* female channel, allowing easy insertion and preventing jamming on the open-end dovetail path.

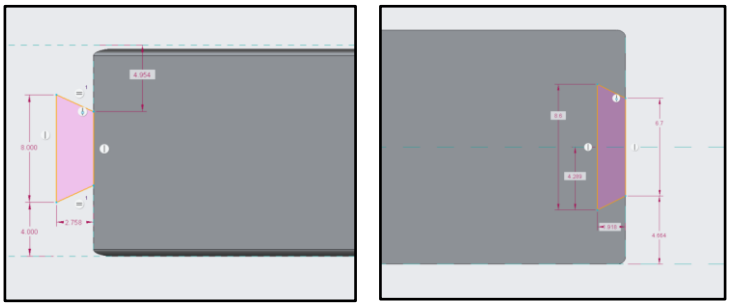

Picture 37. Dovetail dimensions of Part 1(left) and Part 2 (right)

The close-end dovetail track on Part D is designed to prevent the male dovetail of the previous Part D from sliding out during operation. While the Part C has only one female dovetail slot without a male feature, Part D includes both – a central male dovetail and female grooves on either side. The critical design detail is that the female grooves on Part D are at one end, effectively locking the preceding part in place. Because of this, the assembly must begin from the largest part from the right and progress sequentially to the left, thus each male dovetail fully engages before being secured by the closed-end grove of the next part.

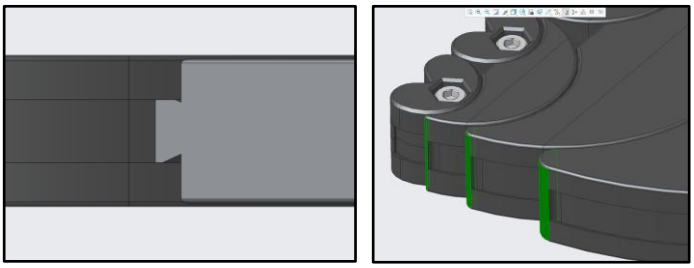

Picture 38. Dovetail insertion mechanism (left) and closed-end paths on female dovetails (right)

One of the parts that can be taken as an example of design process is Part 5, which serves as a Part D and contains two dovetail types. This part is initially sketched with a full circle of *70 mm* diameter. The symmetric fractal shape was then constructed using arc-based cutouts, each with a *35 mm* diameter and centered along the same vertical centerline as the full circle. Unnecessary segments were removed using the *delete segment* feature to shape the double-lobed profile, with the flat back and front surface to accommodate mounting holes. The total length of the flat back surface was dimensioned at *60.32 mm*. with additional features like chamfers, rounds, and holes defined in later steps of model three to complete the component's structure.

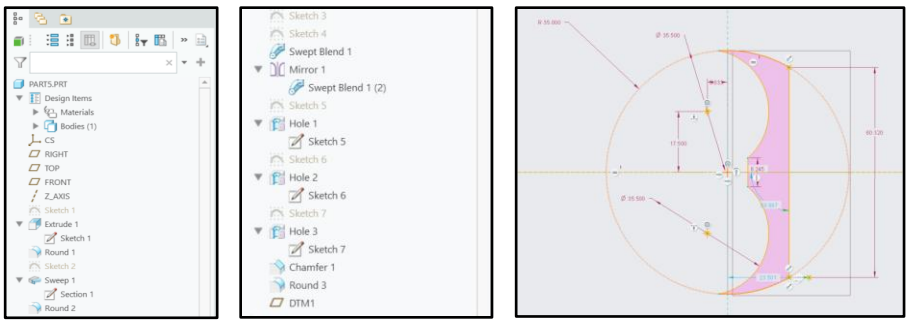

Picture 39. Design features and processes for Part 5

Following the main body, the sweep feature was used to create the female dovetail grooves on each side by sketching the profile on one cutout, requiring two identical end-section sketches and a connecting path. This groove was then mirrored to the opposite side using the vertical mid-plane. The next step involved creating two-hole types: one central hole for an M3 bolt and hex nut, and two smaller holes (Ø2.2 mm, depth 5 mm) on the flat back side for filament insertion. These small holes are essential to restrict the vertical degree of freedom of Part C (which has only one female dovetail).

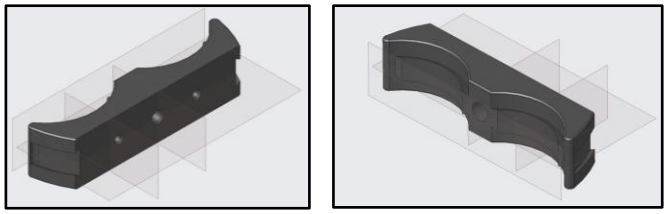

Picture 40. Isometric views of Part 5

Various fasteners and inserts were used in this assembly. The left image shows how brass threaded inserts are embedded into three *Ø6.4 mm* holes on Part 1's backside - slightly smaller than the *Ø8 mm* outer diameter - for an interference fit when melted into the plastic. The internal pitch diameter is *Ø7.2 mm*. The middle figure illustrates the horizontal connection between Part 4 and Part 5 using M3x20 bolts and M3 nuts. Bolt sizes vary (M3x10, M3x12, M3x20, M3x30) depending on location. The right image shows Part 8 connected vertically with M3x12 bolts -12 units are used per side in the Fractal Vise.

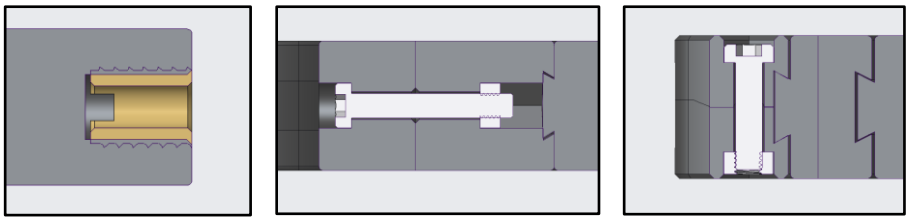

Picture 41. Threaded inserts, bolts, and nuts connections

The assembly drawing of the Fractal Vise shows a combined half-view and half-section top view to illustrate both external form and internal structure. The left side displays the geometry of the fractal components, while the right reveals internal fasteners such as bolts, hex nuts, and brass threaded inserts. The section uses a plastic hatch pattern, indicating PETG-CF as the main material. The full assembly measures *140 mm* (L) × *113 mm* (W) × *16 mm* (H), with Part 1 (the base) at *112 mm* in length. An isometric view aids understanding of fractal scaling. The BOM lists 14 items, including brass inserts (3x), M3 nuts (6x), and four bolt lengths. Items 7–14 are structural/fractal parts, where Part 8 (16x) forms the smallest mirrored clamping teeth.

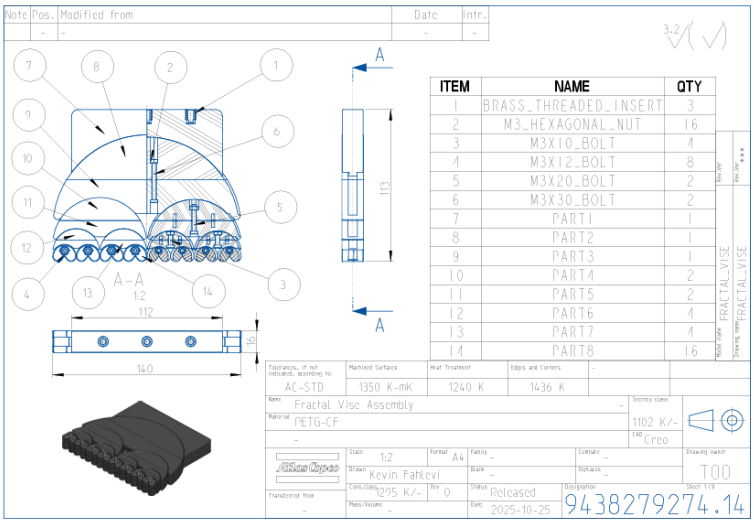

Picture 42. Assembly drawing of the Fractal Vise assembly

5.4 Bench Vise Assembly

The Bench Vise served as the base structure for the hybrid vise assembly, supporting both the frame and mechanical drive. Made of cast steel, it offers high stiffness and durability. It features a fixed and movable jaw operated by a lead screw for linear clamping. Four M8X1.25 threaded holes were used to mount the adaptive Fractal Vise system.

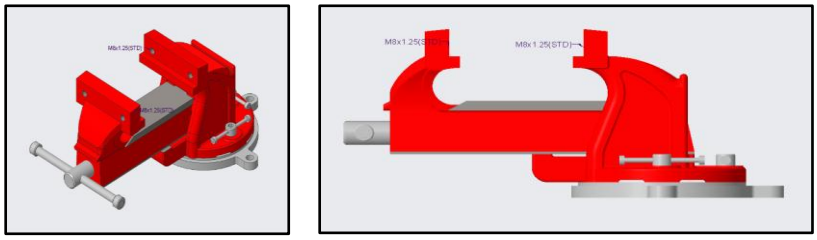

Picture 43. Isometric (left) and side (right) views of the Bench Vise model

The exploded view of the Bench Vise shows its key components: fixed jaw base, movable jaw with slide rail, and rotating base discs (upper and lower swivel plates), and several fasteners. M8X1.25 socket head screws fasten the upper jaw to the rear frame, and a main lead screw with a handlebar and nuts enables actuation. Four M6 bolts secure the base or lock the rotation. The model was assembled in *PTC Creo* using constraints like coincident, parallel, and distance to define part relationships. For example, the sliding jaw was constrained linearly using a distance mate, and the rotating base aligned concentrically. These constraints ensured proper assembly with realistic motion and no interference.

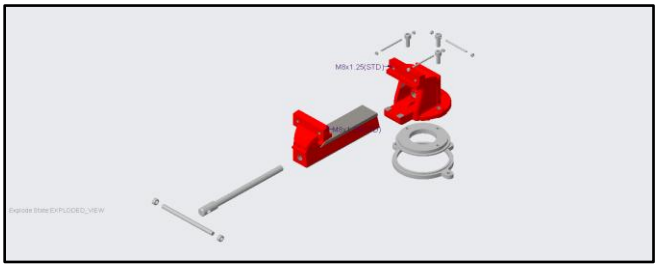

Picture 44. Exploded view model of the Bench Vise assembly

The technical drawing shows the fully assembled Bench Vise, highlighting key dimensions and components with part numbers. The model includes ten parts: jaw inserts, sliding arm, fixed jaw inserts, base plate, support, sliding block, main body, shaft, screws, and a small rod. Key dimensions are: *180 mm* base plate width, *154 mm* mounting hole distance, *135 mm* clamping width, and 38 mm internal clamping depth. The total height is about *141.3 mm*. The base allows rotation, while the main body on the right acts as the central support, made of EN 10293 G20Mn5 cast steel.

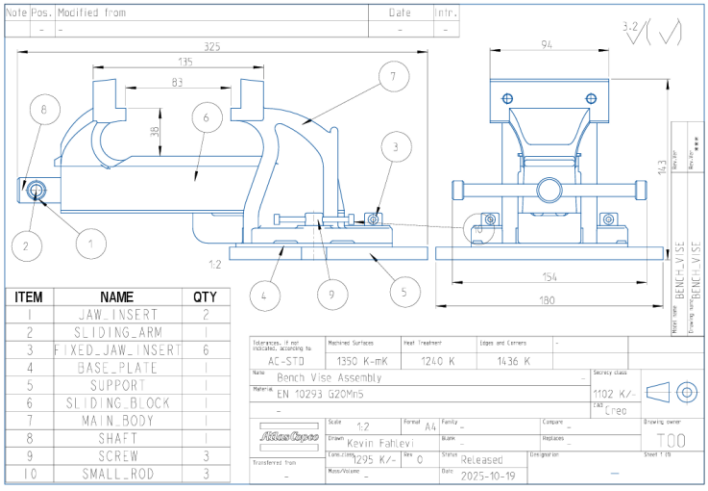

Picture 45. Assembly drawing of the Bench Vise assembly

6. DESCRIPTION OF THE FORMATS

The durability of this integrated vise system on the shop floor depends heavily on material selection, especially for the Fractal Vise's clamping parts, which handle the main load. Key factors included strength, durability, dimensional stability, and wear resistance during clamping. Manufacturing methods for both the fractal components and base plates were also chosen based on these material properties and specific functional needs.

This chapter explains the selected materials – Carbon Fiber Reinforced *PETG* (PETG-CF) for the clamping parts, made by additive manufacturing, and *Aluminum 99.5* for the base plates, made by subtractive methods. Their properties, expected performance, and production steps are discussed accordingly.

6.1 PETG - CF for 3D Printing

PETG-CF has been developed and implemented for a wide range of applications it requires a good balance between mechanical and optical material properties. The raw material is certified according to official standardization: REACH (Registration, Evaluation, Authorization, and Restriction of Chemicals) and RoHS (Restrictions of Hazardous Substances). This type of thermoplastic polymer is reinforced with carbon fibres, but it preserves its natural characteristics as a thermoplastic in a way that it can be repeatedly softened by heating and then solidified by cooling.

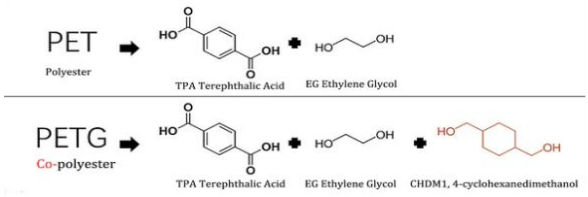

Picture 46. Difference between PET and PETG in terms of chemical structures

PETG is a modified version of *PET*, made by adding CHDM (1,4-cyclohexanedimethanol) to improve ductility, transparency, and thermal processability. While *PET* is strong but brittle, *PETG* overcomes these limitations, making it more suitable for 3D printing applications. When carbon fibers are added into *PETG*, the composite gains significantly improved stiffness, tensile strength, and dimensional stability, at the same time still preserving good printability and layer adhesion and reducing deformation under mechanical load. This explains why *PETG-CF* is an ideal choice for functional prototypes and medium-duty structural components for work holding devices such as the clamping jaws of a Fractal Vise.

Picture 47. Bambu Lab's PETG - CF filament

The mechanical properties of *PETG–CF* show clear anisotropy, with stronger performance in the X-Y direction due to print orientation. According to Bambu Lab **[14]**, Young's modulus in the X-Y plane is about *2460 ± 230 MPa*, roughly double that of standard *PETG*, while in the Z direction it's around *1340 ± 150 MPa*. Tensile strength reaches 35 ± 5 MPa (XY) and *29 ± 4 MPa* (Z), with carbon fiber reinforcement significantly improving modulus and strength compared to unfilled *PETG*. Bending strength is *70 ± 5 MPa* (XY) and *48 ± 4 MPa* (Z), while modulus values are *2910 ± 260 MPa* (XY) and *1560 ± 180 MPa* (Z). Elongation at break is low - especially in Z (4.7 ± 0.4%) - indicating reduced ductility along that axis. Impact strength is higher in X-Y (41.2 ± 2.6 kJ/m²), suggesting good resistance to sudden loads.

Mechanical Properties		
Subjects	**Testing Methods**	**Data**
Young's Modulus (X-Y)	ISO 527, GB/T 1040	2460 ± 230 MPa
Young's Modulus (Z)	ISO 527, GB/T 1040	1340 ± 150 MPa
Tensile Strength (X-Y)	ISO 527, GB/T 1040	35 ± 5 MPa
Tensile Strength (Z)	ISO 527, GB/T 1040	29 ± 4 MPa
Breaking Elongation Rate (X-Y)	ISO 527, GB/T 1040	10.4 ± 0.6 %
Breaking Elongation Rate (Z)	ISO 527, GB/T 1040	4.7 ± 0.4 %
Bending Modulus (X-Y)	ISO 178, GB/T 9341	2910 ± 260 MPa
Bending Modulus (Z)	ISO 178, GB/T 9341	1560 ± 180 MPa
Bending Strength (X-Y)	ISO 178, GB/T 9341	70 ± 5 MPa
Bending Strength (Z)	ISO 178, GB/T 9341	48 ± 4 MPa
Impact Strength (X-Y)	ISO 179, GB/T 1043	41.2 ± 2.6 kJ/m²; 15.7 ±1.6 kJ/m² (notched)
Impact Strength (Z)	ISO 179, GB/T 1043	10.7 ± 1.6 kJ/m²

Picture 48. Mechanical properties of PETG - CF

Due to the anisotropic and layer-dependent strength of 3D-printed parts, *PETG–CF* should be used with a safety factor of at least 2 in load-bearing roles. For example, a part expected to endure *100 N* should be tested to withstand over *200 N*. Engineers often apply this factor to cover dynamic loads and material uncertainties, limiting working stress to around *15–20 MPa* (from 30–

50 MPa ultimate strength). To maximize strength, parts should be printed with critical loads aligned along the fiber-filled XY plane, avoiding reliance on weaker Z-axis bonds **[15]**.

At Atlas Copco Hungary, the *Bambu Lab X1 Carbon* 3D printer is utilized for fabricating functional thermoplastic parts which made for the production line and manufacturing shopfloor, including those made from PETG – CF filament. This advanced printer is equipped with a 0.4 mm nozzle, offers an optimal balance or moderate to high strength between printing speed, surface resolution, and structural integrity. While *0.2 mm* nozzles provide finer detail and *0.6 – 0.8 mm* nozzles deliver faster, stronger prints with rougher surfaces, so overall the *0.4 mm* size is best suited for functional prototyping and tooling needs the company, especially to manufacture this product.

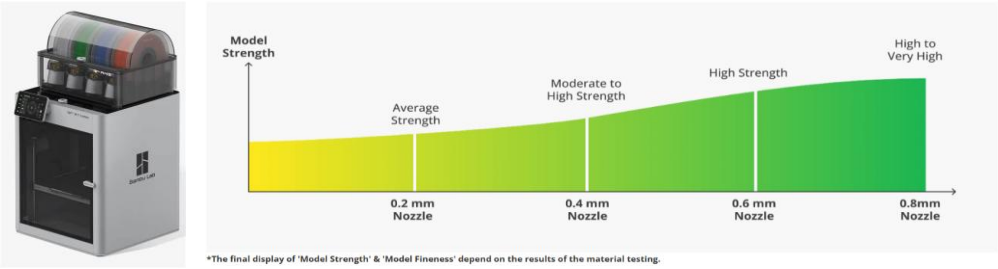

Picture 49. Bambu Lab X1 printer (left) and comparison of different nozzle-types (right)

The development process followed by 3D printing software configurations which involve several precise settings. A total of 20 individual parts is placed on the digital printing board with the automatic and optimized placement orientation; all parts are oriented with their flattest surface against the textured PEI plate, which improves bed adhesion and minimizes the risk of warping or detachment during printing. The other arrangements such as 2 large, curved clamps at the rear of the plate, 6 medium clamps in two rows of three, and 12 small parts are tightly grouped in the front of the plate, arranged in a grid pattern are to support the space utilization and print efficiency while avoiding collision. This setup also allows the printer to reduce travel time between parts.

Under *Quality* tab in the figure below, the layer height is configured to *0.16 mm* for high resolution, and the initial layer height is slightly thicker at *0.2 mm* to ensure strong bed adhesion. Seam position is aligned, and advanced settings enable a cleaner top surface with only one wall. In the *Strength* tab, wall loops are set to 5, and the top/bottom shells are defined with 6 and 4 layers respectively, using a monotonic pattern to improve surface finish. A 50% sparse infill density with

a gyroid patten assures a good balance between strength and material efficiency. Under the *Support* tab, three-style automatic supports are chosen with a threshold angle of 25°, and supports are limited to the build plate only to avoid unnecessary material use.

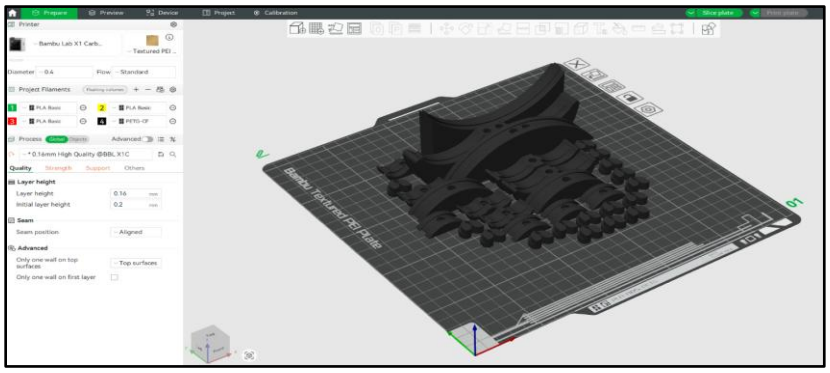

Picture 50. 3D printing layout of Bambu Lab X1 (Quality tab)

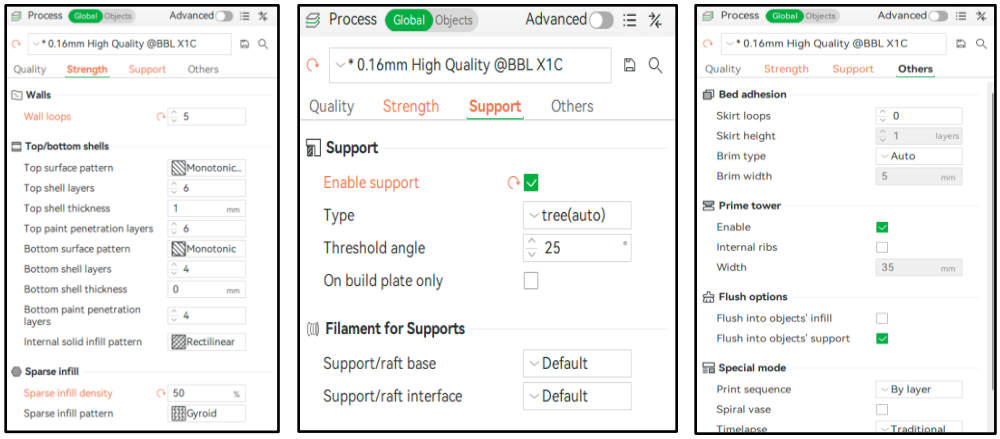

Picture 51. 3D printing configurations (Strength, Support, and Others tabs)

When it comes to the slicing process, the model requires 192.33 g of total filament (one-side of fractal body), with 191.7 g used for the parts and 0.63 g for supports, without any filament change during the process. The estimated print time is 13 hours and 28 minutes, with a total time of 13 hours and 37 minutes including an 8-minute preparation phase. Most time is spent on sparse infill (36.3%) and inner walls (28.4%), followed by outer walls and internal solid infill. The chosen *0.4 mm* nozzle operates across various speeds, from *8 mm/s* for precise movements up to *250 mm/s* for rapid travel paths. These slicing parameters were carefully configured to balance strength, detail, and efficiency for functional mechanical components **[16]**.

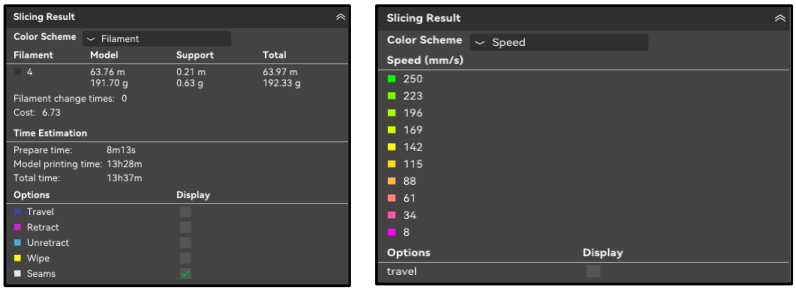

Picture 52. Time estimation and speed variations during slicing

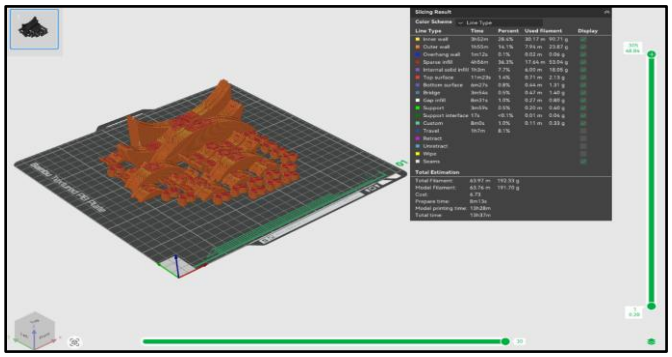

Picture 53. Slicing results of fractal components

After completing the configuration in the *Bambu Studio software*, the selected *PETG – CF* filament was loaded into the AMS (Automatic Material System), and the *Bambu Lab X1 Carbon 3D printer* was prepared for operation. The printer setup included temperature calibration, bed levelling, and final confirmation of slicing parameters. As shown in the picture below, the machine interface displayed the initial printing process. However, at this stage, only a short 1 hour 57-minute print was conducted to produced 2-3 sample parts. This preliminary run served as a test to verify adhesion, support generation, wall quality, and overall compatibility of the slicing settings before proceeding to the full-scale production of the complete batch **[17]**.

Picture 54. 3D printing for the sample fractal components

6.2 Aluminium 99.5 for Milling and Drilling

Delivery condition[5]	Nominal thickness mm		Tensile strength R_m MPa		Elastic limit $R_{p0.2}$ MPa		Elongation % min.		Bending radius[9]		Hardness[9] HBW
	over	to	min.	max.	min.	max.	A50 mm	A	180°	90°	
H14	0,2	0,5	105	145	85	-	2	-	1,0 t	0 t	34
	0,5	1,5	105	145	85	-	2	-	1,0 t	0,5 t	34
	1,5	3,0	105	145	85	-	4	-	1,0 t	1,0 t	34
	3,0	6,0	105	145	85	-	5	-	-	1,5 t	34
	6,0	12,5	105	145	85	-	6	-	-	2,5 t	34
	12,5	25,0	105	145	85	-	-	6	-	-	34
H24	0,2	0,5	105	145	75	-	3	-	1,0 t	0 t	33
	0,5	1,5	105	145	75	-	4	-	1,0 t	0,5 t	33
	1,5	3,0	105	145	75	-	5	-	1,0 t	1,0 t	33
	3,0	6,0	105	145	75	-	8	-	1,5 t	1,5 t	33
	6,0	12,5	105	145	75	-	8	-	-	2,5 t	33
O / H111	0,2	0,5	65	95	20	-	20	-	0 t	0 t	20
	0,5	1,5	65	95	20	-	22	-	0 t	0 t	20
	1,5	3,0	65	95	20	-	26	-	0 t	0 t	20
	3,0	6,0	65	95	20	-	29	-	0,5 t	0,5 t	20
	6,0	12,5	65	95	20	-	35	-	1,0 t	1,0 t	20
	12,5	80,0	65	95	20	-	-	32	-	-	20
H112	≥ 6,0	12,5	75	-	30	-	20	-	-	-	23
	12,5	80,0	70	-	25	-	-	20	-	-	22
[5]	Other possible delivery conditions for this alloy: H12 · H16 · H18 · H19 · H22 · H26 · H28										
[9]	For information only										

Picture 55. Mechanical strengths of Aluminum 99.5 sheet/plates

Aluminum 995% (EN AW 1050A) is a high-purity, non-heat-treatable alloy known for its corrosion resistance, high electrical and thermal conductivity, and good formability. It contains at least 99.5% aluminum with small traces of Fe (≤0.4%), Si (≤0.25%), and others (≤0.05%). In the O (annealed) temper, it is soft and ductile with *65–95 MPa* tensile strength, *20 MPa* yield strength, and 20–35% elongation. The H14 (half-hard) condition offers a balance of strength and formability, with *105–145 MPa* tensile and *85 MPa* yield strength, but only 2–6% elongation. The H24 (strain-hardened) temper provides *105–145 MPa* tensile and up to *75 MPa* yield strength, with 3–8% elongation. Hardness ranges 20–34 HBW. The H18 temper gives maximum strength and minimum ductility **[18]**.

Specifications in % Remainder: Aluminium												Other	
Si	Fe	Cu	Mn	Mg	Cr	Ni	Zn	Ti	Ga	V	Note	Individual	Total[2]
0,25	0,40	0,05	0,05	0,05	-	-	0,07	0,05	-	-	-	0,03	-
[X]	Chemical specifications as perc. of weight. If no ranges are specified, the alloy content has the maximum value.												
[2]	Includes all items listed for which no limit values are specified.												

Picture 56. Chemical composition of Aluminum 99.5

Aluminum 99.5 is easy to shape, cut, and machine due to its high ductility and purity. Grades like 1050/1100 are ideal for deep drawing or spinning. While pure aluminum is simple to machine, it may cause built-up edges without proper lubrication. Cold-worked tempers like H14/H18 machine better with carbide tools. In softer states, it can stick to cutters, so sharp tools, high speeds, and cutting fluids are recommended. Though not as free machining as alloys like 6061

or 2011, 99.5% of Al still performs well in CNC operations. Swarf can be persistent, and thread tapping requires care to avoid galling or shearing from shallow engagement **[19]**.

Picture 57. Aluminum 99.5 plate/sheet

Alongside the additive manufacturing of fractal components, the mounting interface plates were produced through subtractive manufacturing using *Aluminum 99.5* as the base material. At Atlas Copco Hungary, two machines are used for milling and drilling. The first, INTOS FNGJ 40 (by INTOS spol. s.r.o.), is a universal milling machine for vertical and horizontal operations. It has a swiveling spindle head, tilting ram, and an *800 × 400 mm table*, with stepless spindle speeds via a 2-step frequency converter, reaching up to 4000 RPM **[20]**.

The machine is equipped with hardened guideways for long-term durability, central lubrication via dosing devices for smooth operation, and hand wheels with fine *0.01 mm* divisions in X, Y, and Z axes for precise manual positioning. Cooling systems are integrated, although the standard execution uses manual tool clamping, optional upgrades allow for pneumatic-hydraulic tool clamping in both vertical and horizontal spindles. With its compact layout, oil resistant surface paint, and reliable electrical system (3x400V, 50 Hz), this machine is appropriate for a standard application at the maintenance or manufacturing shopfloor.

Picture 58. Manufacturing machine used for milling processes

The second machine, the Bridgeport Series I, is a precision knee-type vertical milling machine by Bridgeport (Hardinge Inc.). It has a 9”×49” (229×1245 mm) worktable with travels of 36” (X), 12” (Y), and 16” (Z), plus a quill travel of 5” (127 mm) for fine depth control. Driven by a 2 HP continuous motor (3 HP peak), the spindle runs between *60–500 RPM* and *500–4200 RPM*, suitable for various drilling and light milling tasks. It uses an R-8 taper, manual handwheels with *0.01 mm* precision, hardened guideways, one-shot lubrication, and a cast-iron body **[21]**.

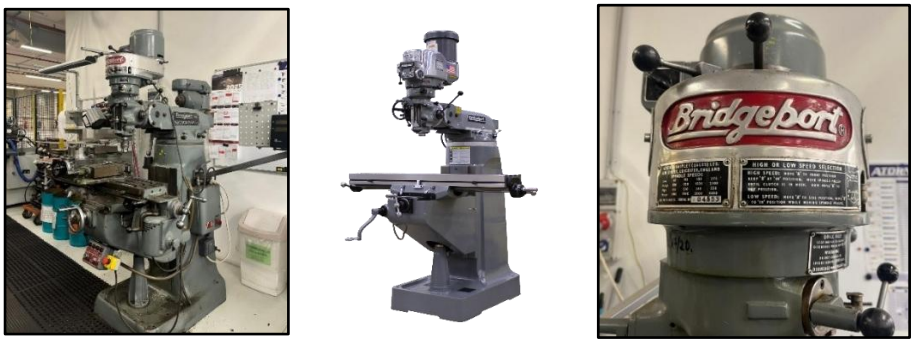

Picture 59. Milling machine Bridgeport Series I

Initial milling was performed using various tools mounted on the FNGJ 40 to shape the aluminum plates. Tools included face mills for large flat surfaces, end mills for pocketing and contouring, and chamfer mills for edge finishing. With full XYZ movement, rough and fine milling were completed efficiently by the maintenance operator at Atlas Copco.

Following the milling stage, the prepared plates were transferred to the *Bridgeport Series I*. The drilling process began with a centre drill to precisely locate the hole position, followed by a *Ø4.2 mm* drill bit for M5 tapping holes and a *Ø5.2 mm* drill for a through-hole. A countersink tool was then used to create a chamfer at the hole entrance, easing the threading process with hand taps for both M5 and M8 threads. Lastly, another chamfering operation was applied to smooth both ends of the threaded holes.

Picture 60. Collection of milling (left) and drilling (right) tools used for the mounting interface plates – left to right order

7. INDUSTRIAL CAPABILITY

The experimental testing examined the vise assembly's performance under realistic workshop conditions, focusing on clamping strength, stability, and usability. The first model, without the cap plate, was tested using three workpieces - a cutting plier, socket wrench handle, and ratchet torque wrench. During testing, all clamping teeth (Part 8) were observed to move and adapt to the workpiece surface as torque was applied on the Bench Vise handle. This torque generated linear force across the fractal components, allowing the clamping system to adjust dynamically. In observations, the vise modified symmetrically to match the convex geometry of certain tools, where both sides mirrored each other. In contrast, for more complex shapes like the socket wrench handle, it showed asymmetrical adaptation - the blue side aligned with the straight shaft while the black side adjusted to the wider wrench head.

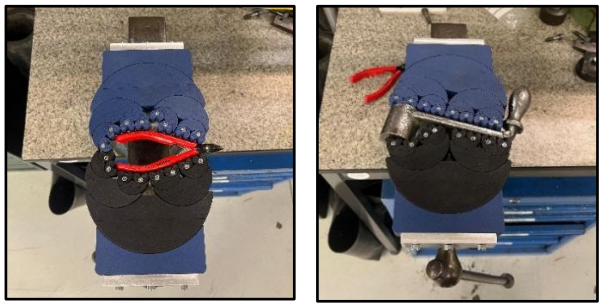

Picture 61. First model of Fractal Vise testing on cutting plier (left) and socket wrench handle (right) – top views

The clamping test was extended to a larger tool, a *420 mm* ratchet torque wrench, while the Fractal Vise front covered about one-third of its length - exceeding the vise's own size. Despite this scale difference, both the black and blue teeth are symmetrically adjusted to grip the wrench's curved head, proving this typical vise system also works with large-shaped tools.

Picture 62. Fractal Vise testing on large tool (ratchet torque wrench) - isometric view

During further testing of the Fractal Vise, a mechanical limitation was observed, as shown in the images below. In the left picture below, when clamping a workpiece, the blue side (left body) displays a noticeable upward bending near the bottom section, whereas the black side (right body) remains aligned with the horizontal plane of the mounting plate (Part 2). The deformation on the blue side begins at Part 2 and visibly affects the left portion of the entire vise. The bending deviation appears to be approximately *2.5 mm* to *3 mm* at its peak, particularly on the lower edge. From a mechanical perspective, this asymmetric deformation occurs because the blue side is connected to the fixed jaw of the Vise, which is subjected to reaction forces when clamping pressure is applied. On the other hand, the black side is supported by the moving jaw, which travels to apply pressure but is not structurally restrained which push freely without resistance. This means the fixed side must absorb both the clamping reaction force and potential torsional moments from the shifting load, leading to upward flexing if the material lacks sufficient stiffness. The right image reveals this bending effect in closer view: the horizontal alignment is disrupted, and the blue body tilts upward due to local deflection under concentrated stress **[22]**.

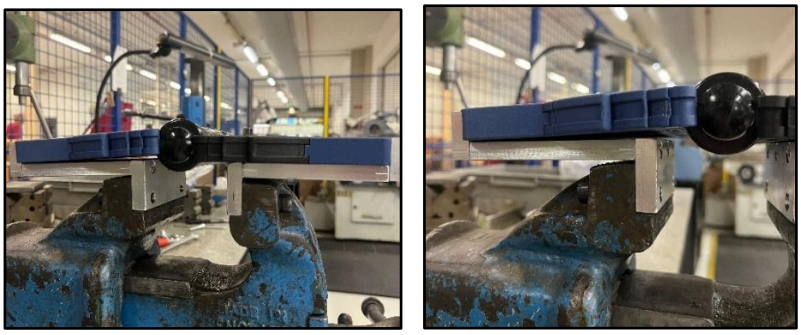

Picture 63. Observed bending during the application trial of first model – side views

Following the previous observation of bending deformation in the initial vise integration model, a second stage of experimental testing was conducted using an upgraded version that includes an additional cap plate. Five different tools were tested, arranged from simplest (left) to most complex (right) in shape; a rectangular steel block, a quick-release hydraulic connector, a *13 mm* wrench, a water hose connector (with a brass thread and plastic nozzle), and a heavy-duty ball valve. In each case, the clamping teeth of the Fractal Vise automatically adjusted to match the varying geometries of the objects. For adjustments the wrench and valve were clamped effectively, where 47 symmetrical adjustments of both clamping sides were created and independently secure contact with their sur faces.

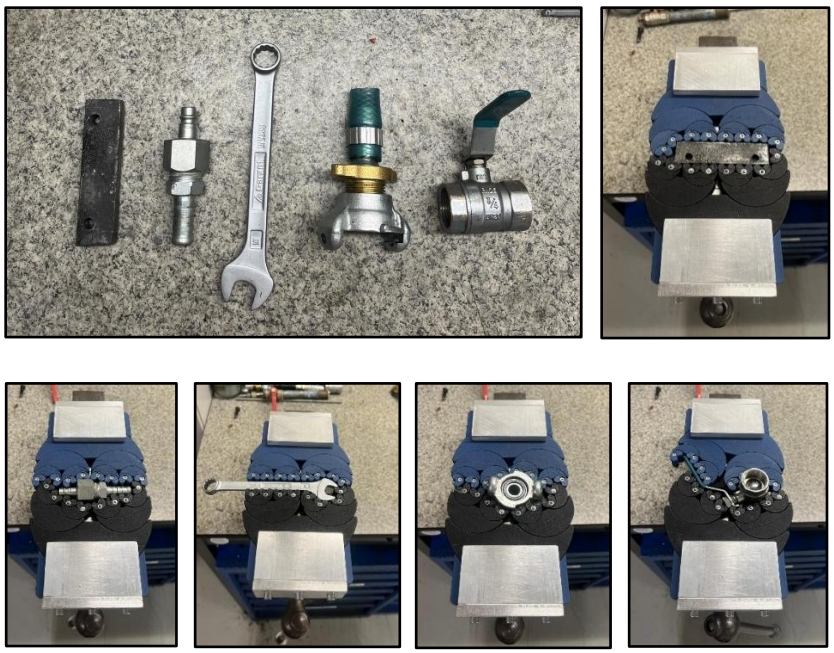

Picture 64. Second model of Fractal Vise testing on five different tools – top views

The side view photos show improved structural stability in the upgraded Fractal Vise. A cap plate spanning half the vise length - covering the dovetail section of Part 2 - significantly reduced the flexural deformation seen in the earlier model. With the same torque applied, both clamping sides stayed aligned with the base and showed no upward deflection. This improvement is due to an increased second moment of area (moment of inertia), which governs flexural stiffness. Since the second moment of area, I for a rectangular cross-section is proportional to the cube of its height h (I = 12bh3), even a small increase in height leads to a substantial increase in stiffness. Compared to the original configuration without the cap, the addition of a 10 mm-tall cap over a *52 mm* span results in an approximate increase in bending stiffness by up to 300-4005 in the rain forced region. This effectively redistributes the clamping stress across a larger area and restrains 48 vertical deflections, thereby eliminating the initial flexural failure seen at the unreinforced first model.

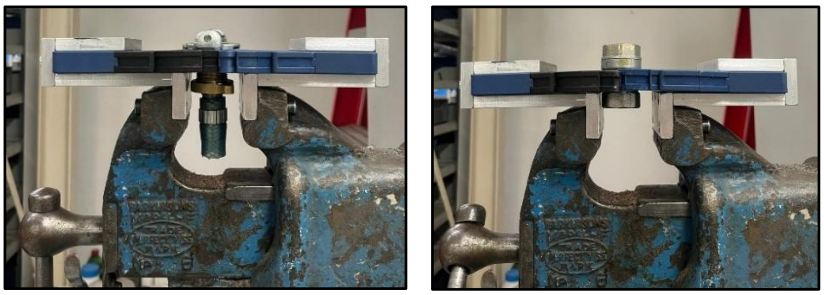

Picture 65. Second model of Fractal Vise testing on water hose connector (left) and ball valve (right) - side views

8. MARKET ANALYSIS

The proposed integration model of Fractal Vise and Bench Vise (hybrid Fractal Vise) targets small to medium-sized workshops and makerspaces where optimization and efficient tool handling are prioritized. This segment continues to grow with the increasing adoption of 3D printing and digital fabrication technologies across industries. This chapter will present the current trends, inside-sales opportunities, utilization risks and alternative solutions **[23]**.

81. Market Opportunities

Globally, the market for metalworking vises is expected to reach a valuation of more than USD 1.5 billion, with a growth rate of 5.2°yearly. Fractal Vises are growing at a 6.2% CAGR through 2028, driven by automation trends and demand for high precision, multi-axis machining solutions, especially those with metal-base material. Asia-Pacific leaks distribution, with China producing 58% of global supply. There is a steady market demand for modular and lightweight vise models, especially in the aerospace, electronics, and medical device sectors. Other significant players include Germany, Japan, and the US, focusing on multi-axis variants. Notable industry trends include **[24]**:

- 5-axis capable vises make up 40% of new product launches.
- Self-centering mechanisms are featured in 78-85% of premium grade offerings.
- New designs are increasingly light - 22% lighter – due to composite alloys, without sacrificing structural integrity.
- IoT integration has been adopted in 15% of high-end vises, for real-time clamping pressure monitoring.

Chinese market players in the field of clamping-technologies solutions such as Kamishiro **[25]**, Shenzhen Jingzuan **[26]**, and Dezhou Panda **[27]** offer modular systems made of metal and aluminum base materials with reorder rates exceeding 25% of high buyer retention. Depending on complexity and features, pricing ranges widely – from $450 to over $600 for various types of clamping designs, jaw structures, and power mechanisms.

On the other hand, sales opportunities could be potentially strong in the educational (technical universities) and prototyping sectors (R&D labs), where batch production is low volume but highly favored, additionally lightweight design and compact model which are reliable for learning opportunities. As the global market for 3D printed tooling is projected to exceed USD 5 billion by 2030, functional tools like custom jigs and vises comprising a steadily increasing share and application, considering the special preference of hybrid integration into Bench Vise which leads to more affordable market prices – ranges starting from $200 - $250/unit. Assuming an annual adoption rate of 500 units of 3D printed vises within small fabrication hubs across Europe, and a modest price point of $300 each, the potential revenue could reach $150,000 (gross revenue exclude manufacturing cost) in early-stage commercialization **[28]**.

From the perspective of Atlas Copco Hungary **[29]**, the 3D printed hybrid vise model was developed to enhance the operational efficiency on the shopfloor, especially the technicians working on daily tool maintenance or assembly setups. The vise eliminates the need for frequent tool changes and simplifies work holding for Atlas Copco various spare parts, such as GTG motors, power couplings, pinion pullers, stator casing, test adaptor, power shaft, etc. Operators benefit from its adaptability, especially when assembling those spare parts onto the finish goods - for instance FTM-32 Fixed Bolt Tightener Module, HTM-32 Manual Screw Feeder Module, Tensor ES Corded Straight Screwdriver, Tensor ES Corded Pistol Grip Screwdriver, MWR Mechatronics Torque Wrench – where they are vary in size and form, and the vise helps reduce setup time and tool-switching frequency by 15 – 20% and spatial installation footprint by ~25%.

Picture 66. HTM-32 Manual Screw Feeder Module (left) and Tensor ES Corded Pistol Grip Screwdriver (right)

8.2 Challenges and Solutions

The primary application of this hybrid model of Fractal Vise is in maintenance workshops and assembly lines, particularly in environments where manual handling and light-machining tasks dominate. While the clamping area of the installation at Atlas Copco Hungary is measured – approximately *161 mm* in length and *130 mm* in width – the ideal examined tools shall be with a smaller dimension, to create a strong gripping force. However, it is possible to secure larger objects, but the clamped portion must still conform within the vise's available contact dimensions.

Competition between conventional metal vises and 3D printed vises may challenge the pricing strategy. As the hybrid Fractal Vise developed with metal base materials (e.g. Aluminum, mild streel) exhibits superior material strength, durability, and thermal resistance – this make is suitable for repeated daily use in industrial metal machining tasks where super clamping force is frequently required. On the other hand, 3D printed Fractal Vise could be manufactured from PLA, ABS, PETG filaments which are generally intended for prototyping, educational use, or demonstration purposes for low load holding tasks. Therefore, pricing range for metal base hybrid vises ($400 - $550) is higher by around 2-3 times of the 3D printed vise ($200-$350) as CNC manufacturing is required to create metal fractal bodies. These prices differ and exclude the manufacturing cost of mounting interface plates, thus still slightly lower than a fully Fractal Vise model.

Due to its size and material selection, this typical vise may not directly compete in the high-end CNC compatible vise market, as it is not ideal for high-load applications typically found in full-scale manufacturing lines. These lines rely on advanced clamping devices integrated with hydraulic, pneumatic or automated robotic systems. Nevertheless, its ease of integration in various vises, minimal part count, and modularity open opportunities for scaling, particularly in developing markets or for firms optimizing lean manufacturing setups. Potential adaptations – like increased clamping with or added self-centering mechanism – could further expand its commercial value **[30]**.

9. BUSINESS PLAN

Material	Supplier	Source	Market Price [Currency]	Quantity [Unit]	Used Quantities [Unit]	End Price [Currency]
Aluminium 99.5	Alucentrum	Link 1	12192 [HUF]	100x 10 [mm] - 1 [m]	94x10 [mm] - 0.423 [m]	5157 [HUF]
PETG - CF	3D Jake	Link 2	15590 [HUF]	1000 [g]	384.66 [g]	5997 [HUF]
M3x10 Bolts	Szogker	Link 3	18 [HUF]	1 [PCS]	8 [PCS]	144 [HUF]
M3x12 Bolts	Szogker	Link 4	52 [HUF]	1 [PCS]	16 [PCS]	832 [HUF]
M3x20 Bolts	Szogker	Link 5	24 [HUF]	1 [PCS]	4 [PCS]	96 [HUF]
M3x30 Bolts	Szogker	Link 6	30 [HUF [	1 [PCS]	4 [PS]	120 [HUF]
M3 Hex Nuts	Szogker	Link 7	5 [HUF]	1 [PCS]	32 [PCS]	160 [HUF]
M5x20 Countersink Screws	Szogker	Link 8	25 [HUF]	1 [PCS]	9 [PCS]	225 [HUF]
M5x16 Hex Socket Head Screws	Szogker	Link 9	110 [HUF]	1 [PCS]	6 [PCS]	660 [HUF]
M8x25 Hex Socket Head Screws	Szogker	Link 10	70 [HUF]	1 [PCS]	4 [PCS]	280 [HUF]
M5X10 Threaded Inserts	Szogker	Link 11	90 [HUF]	1 [PCS]	6 [PCS]	540 [HUF]
Material Cost						**14211 [HUF]**

The hybrid Fractal Vise prototype was developed using minimal material resources, utilizing thermoplastic *PETG-CF* and *Aluminum 99.5*, both sourced locally in Hungary. Since the model was mounted on an existing Bench Vise, no additional cost was incurred for the base. A 423 mm section of aluminum flat bar (100x10 mm) was used, costing 5,157 HUF, while approximately 385 g of PETG-CF filament was consumed at 5,997 HUF. Fasteners and inserts totaled 3,057 HUF, which resulted in the total material cost to 14,211 HUF, equivalent to $42.21 per hybrid vise unit **[31] [32]**.

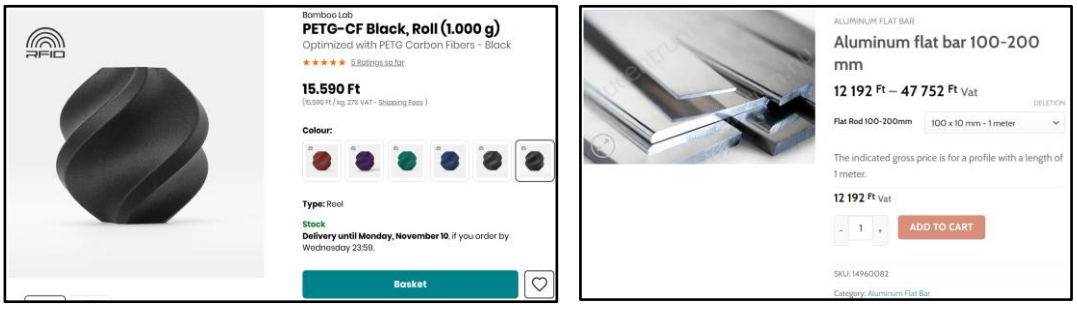

Picture 67. Material cost for PETG-CF (left) and Aluminum 99.5 (right) from Atlas Copco's supplier

In terms of manufacturing/labor cost, subtractive operations (such as manual milling and drilling) were used on the aluminum parts (8 parts in total), taking approximately 1.5 hours, with a local labor cost estimate of 3,800 HUF/hour. This results in a labor cost of 5,700 HUF. The 3D printing of thermoplastic parts using *PETG-CF* required around 13 hours 37 minutes for fractal components of one body, so 27 hours and 14 minutes for total required fractal parts, with a typical 3D printer operating at 1,500 HUF/hour, which is calculated to 40,850 HUF in total for printing cost. Thus, the total estimated labor cost is 46,550 HUF, equal to €120.5 per hybrid vise unit. In sum, the full prototype cost (materials + labor) is around 60,671 HUF ($180).

Assume the price per unit is $300 and 500 units sold annually, the hybrid Fractal Vise may target small-medium scale markets like maintenance workshops, assembly lines, and research labs. Below is the profit calculation:

$$Total\ revenue\ before\ cost = 500\ units\ x\ \$300 = \$150{,}000$$

$$Total\ manufacturing\ cost = 500\ units\ x\ \$222 = \$111{,}000$$

$$Net\ yearly\ revenue\ (profit) = \ \$150{,}000 - \ \$83{,}000 = \ \$39{,}000 \sim 13{,}131{,}000\ HUF$$

Assuming an annual sales volume of 500 units at a price of $350 each, the total revenue would reach $175,000. With the same estimated manufacturing cost per unit, the total production expense would be $111,000, resulting in a net yearly profit of approximately $64,000, or around 21.5 million HUF.

Since the concept is based on integrating the Fractal Vise mechanism into existing industrial vises, the product is not limited to Bench Vises; it can also be adapted to Machine Vises and Quick-Release Vises by customizing the mounting interface according to its jaw space and user requirements. This flexibility shifts the business from selling standard products (traded goods) to a contract manufacturing model, where designs, materials, and manufacturing are tailored to specific industrial clients. The standardized dimensions of industrial vises make it feasible to scale customization without major design overhauls. Variants – for instance bearing-supported jaws, flexure-based designs, or different jaw profiles (flat, c-shaped, curved) – can be offered depending on customer needs.

10. CONCLUSION

The hybrid Fractal Vise was developed as a novel clamping solution aimed at enhancing versatility, efficiency, and adaptability in maintenance workshops and light assembly environments, particularly at Atlas Copco Hungary. The core idea focused on modular integration – where the fractal jaws and interface plates are mounted onto existing vise bases – minimizing material usage and production cost, additionally improved streamlined clamping operation by 18% and spatial installation footprint by ~25 %. The development progressed through CAD design and modeling via *PTC Creo*, structural planning, material analysis of both *PETG-CF* and *Aluminum 99.5* along with the additive manufacturing and subtractive manufacturing, respectively. Prototypes were tested within the Atlas Copco Hungary workshop, successfully clamping various tool geometries including irregular industrial components. These proof-of-concept trials confirmed the vise's ability to handle light machining tasks, providing strong grip, ergonomics function, and adaptability in real industrial conditions.

From a market perspective, the hybrid Fractal Vise targets small to medium-scale industries where flexibility and customization are valued. The business model transitions from selling standard conventional vise into a modular solution of hybrid vise – adapting fractal jaw types, mounting interfaces, and geometries to fit different industrial vise bases such as Bench Vise, Machine Vise, and Quick-Release Vise. This contract-manufacturing strategy allows the product to serve multiple sectors with standardized ideas or concepts, but customizable designs. Financial estimates show promising returns, with a potential net yearly profit of $64,000 (≈21.5 million HUF) from 500 units sold at $350 each. The project demonstrates strong business feasibility for commercialization with scalable production paths and relevance in modern lean-manufacturing environments.

BIBLIOGRAPHY

[1]. Jiaxin Huang, Jian Shen, Yilin Zheng, Zhigong Song, “Fractal Gripper: Adaptive manipulator with mode switching,” (accessed on Sept 3rd 2025). [Online]. In: Cornell University, Computer Science and Robotics. Available: [2402.16057] Fractal Gripper: Adaptive manipulator with mode switching

[2]. Tran Thanh Tung and Tran Vu Minh, “Development of a Prototype Fractal Vise,” (accessed on Sept 12nd 2025). [Online]. In: International Journal of Mechanical Engineering and Robotics Research, Vol. 14, No. 1, (2025), pp. 11-12. Available: Development of a Prototype Fractal Vise

[3]. Engineers Edge, LLC, “Coefficient of Friction Equation and Table Chart,” (accessed on Sept 13th 2025). [Online]. Available: Coefficient of Friction Equation and Table Chart

[4]. Christopher Borge, “3D Print A Fractal Vise That Can Hold Odd Shapes,” (accessed on Sept 15th 2025). [Online]. Available: 3D Print A Fractal Vise That Can Hold Odd Shapes - Make:

[5] BubsBuilds, “Fractal Vise Jaws - Mechanical Bearings,” (accessed on Sept 17th 2025). [Online]. Available: Fractal Vise Jaws - Mechanical Bearings

[6]. Jiaxin Huang, Jian Shen, Yilin Zhemg, Yanbo Guo, and Zhigong Song, “A fractal gripper with switchable mode for geometry adaptive manipulation,” (accessed on Sept 17th 2025). [Online]. In: Sci Rep 15, 14657 (2025). Avaiable: https://doi.org/10.1038/s41598-025-98752-z

[7]. P. O'Brien, J. F. Kowalewski, C. C. Kessens and J. I. Lipton, "A Fractal Suction-Based Robotic Gripper for Versatile Grasping," (accessed on Sept 19th 2025). [Online]. In: IEEE Robotics and Automation Letters, vol. 9, no. 7, pp. 6208-6215, (July 2024), doi: 10.1109/LRA.2024.3401138. Available: A Fractal Suction-Based Robotic Gripper for Versatile Grasping | IEEE Journals & Magazine | IEEE Xplore

[8]. Mr. Shrikant M. Chougule, Prof. D. B. Waghmare, “Design & Manufacturing of Components of Modified Bench Vise on Rapid Prototype Machine,” (accessed on Sept 20th 2025). [Online]. In: International Journal of Application or Iinnovation in Engineering & M management (IJAIEM), vol. 4 (7 July 2015). ISSN 2319 – 4847. Available: Prensa_de_banco_materiales-libre.pdf

[9].Essam Ali Al-Bahkali, Adel Taha Abbas, “Failure analysis of vise jaw holders for hacksaw machine,” (accessed on Sept 21st 2025). [Online]. In: Journal of King Saud University – Engineering Science, vol 30, (2018), pp68-77. Available: Failure analysis of vise jaw holders for hacksaw machine

[10]. J. W. Burdick and M. Tisdale, "The Fractal Hand–I: A Non-anthropomorphic, but Synergistic, Adaptable Gripper," (accessed on Sept 22nd 2025). [Online]. In: 2024 IEEE International Conference on Robotics and Automation (ICRA), Yokohama, Japan, (2024), pp. 4162-4169, doi: 10.1109/ICRA57147.2024.10610687. Available: The Fractal Hand–I: A Non-anthropomorphic, but Synergistic, Adaptable Gripper | IEEE Conference Publication | IEEE Xplore

[11]. M. Tisdale and J. W. Burdick, "The Fractal Hand-II: Reviving a Classic Mechanism for Contemporary Grasping Challenges," (accessed on Sept 23rd 2025). [Online]. In: 2024 IEEE International Conference on Robotics and Automation (ICRA), Yokohama, Japan, (2024), pp. 4133-4139, doi: 10.1109/ICRA57147.2024.10611267.

[12]. M. O. Idris, K.M. Adeleke, I.K. Okediran, and T.I. Mohammed, “Design and Fabrication of a Modified Bench Vise for Comfortability and Productivity,” (accessed on Sept 26th 2025). [Online]. In: Adeleke University Journal of Engineering and Technology, Vol. 5, No. 1, (2022), pp. 01-07. Available: View of Design and Fabrication of a Modified Bench Vise for Comfortability and Productivity

[13]. Mr. R. Rupanawar, Mr. T. V. Daundkar, Mr. S. R. Tanpure, and Prof. V. V. Said Patil, “Design and Modification of Bench Vice by Increasing the Degrees of Freedom,” (accessed on Sept 27th 2025). [Online]. In: GRD Journals- Global Research and Development Journal for Engineering, vol. 1, (11 October 2016), ISSN: 2455-5703. Available: GRDJEV01I110053_OK-libre.pdf

[14]. Spectrum Filaments, “THE FILAMENT PETG CF,” (accessed on Sept 28th 2025). [Online]. Available: eng_tds_the_filament_petg_cf.pdf

[15]. Bambu Lab, “PETG-CF,” (accessed on Oct 2nd 2025). [Online]. Available: Bambu_PETG-CF_Technical_Data_Sheet_V2.pdf

[16]. M. Viccica, M. Galati, F. Calignano, L. Iuliano, “An additively manufactured fractal structure for impact absorption applications,” (accessed on Oct 5th 2025). [Online]. In: Procedia CIRP. 118,

793-798 (2023). Available: An additively manufactured fractal structure for impact absorption applications - ScienceDirect

[17]. Y. Sun, Y. Liu, F. Pancheri, T. C. Lueth, "LARG: A Lightweight Robotic Gripper With 3-D Topology Optimized Adaptive Fingers," (accessed on Oct 9th 2025). [Online]. In: IEEE/ASME Transactions on Mechatronics. 27, 2026-2034 (2022). Available: 2402.16057

[18]. Bikar Metals, "EN AW-1050A". [Online]. Available: Aluminium ::: EN AW-1050 A

[19]. Pinkham, Myra, "The future of aluminum manufacturing," (accessed on Oct 11st 2025). [Online]. In: ProQuest, Redhill Vol. 32, Iss. 2, (Mar/Apr 2019): 21-23. Available: The future of aluminium manufacturing - ProQuest

[20]. TOS OLOMOUC s.r.o, "Tool-room milling machine FNGJ 40 A," (accessed on Oct 14th 2025). [Online]. Available: Tool-room milling machine FNGJ 40 A - TOS Olomouc s.r.o.

[21]. Bridgeport, "SERIES 1 BRIDGEPORT MILL," (accesses on Oct 14th 2025). [Online]. Available: Bridgeport® Series I Standard Knee Mill

[22]. Dina Rochman and Sergio Vásquez, "A Conceptual Framework Based on Fractal Geometry for Design, Modeling and Rapid Prototyping of Complex Geometric Shapes," (accessed on Oct 18th 2025). [Online]. In: Computer-Aided Design and Applications, 10(2), pp. 307–319. https://doi.org/10.3722/cadaps.2013.307-319. Available: A Conceptual Framework Based on Fractal Geometry for Design, Modeling and Rapid Prototyping of Complex Geometric Shapes: Computer-Aided Design and Applications: Vol 10, No 2

[23]. R. Magdalena et al. (eds.), "Comprehensive Market Analysis and Assessment: Unveiling Trends and Strategies for Future Growth," (accessed on Oct 20th 2025). [Online]. In: Proceedings of the 2024 9th International Conference on Social Sciences and Economic Development (ICSSED 2024), Advances in Economics, Business and Management Research 289, https://doi.org/10.2991/978-94-6463-459-4_29. Available: 126001646.pdf

[24]. Verified Market Reports, "Metalworking Vise Market Insights," (accessed on Oct 24th 2025). [Online]. Available in: Metalworking Vise Market Size, Competitive Dynamics, Growth & Forecast 2033

[25]. Kamishiro Tools (dongguan) Co., Ltd., “16 YEARS CLAMPING SYSTEMS,” (accessed on Nov 1st 2025). [Online]. Available: Company Overview - Kamishiro Tools (dongguan) Co., Ltd.

[26]. Shenzhen Jingzuan Intelligent Manufacturing Co., Ltd., “25 years professional manufacturing,” (accessed on Nov 3rd 2025). [Online]. Available: Company Overview - Shenzhen Jingzuan Intelligent Manufacturing Co., Ltd.

[27]. Dezhou Panda Machinery Co., Ltd., “25 years professional manufacturing,” (accessed on Nov 3rd 2025). [Online]. Available: Vise Series-Panda-tool

[28]. Etsy, “Fractal Vise 3D Print,” (accessed on Nov 4th 2025). [Online]. Available: Fractal Vise 3d Print - Etsy Italy

[29]. Atlas Copco Hungary, “Industrial Tools & Solutions,” (accessed on Nov 4th 2025). [Online]. Available: Assembly tools & solutions - Various assembly solutions for your needs

[30]. Praveena B.A, Lokesh N, Abdulrajak Buradi, Santhosh N, Praveena B L, Vignesh R, “A comprehensive review of emerging additive manufacturing (3D printing technology): Methods, materials, applications, challenges, trends and future potential,” (accessed on Nov 4th 2025). [Online]. In: materialstoday: PROCEEDINGS, vol. 52, Part 3, (2022), pp. 1309-1313. Available: A comprehensive review of emerging additive manufacturing (3D printing technology): Methods, materials, applications, challenges, trends and future potential - ScienceDirect

[31]. 3D JAKE, “Bamboo Lab (PETG-CF Black, Roll (1.000 g),” (accessed on Nov 4th 2025). [Online]. Available: Bamboo Lab PETG-CF Black - 3DJake Online Shop

[32]. Alucentrum, “Aluminum flat bar 100-200 mm,” (accessed on Nov 4th 2025). [Online]. Available: https://alucentrum.hu/aluminium-profil-arak/aluminium-lapos-rud-arak/aluminium-lapos-rud-arak-100-150-mm/